Alma Mater Studiorum · Università di Bologna

Scuola di Scienze
Corso di Laurea in Fisica

Dielectric Relaxation in Biological Materials

Relatore:
Prof. Francesco Mainardi

Presentata da:
Eleonora Barelli

Sessione II
Anno Accademico 2014/2015

Abstract

The study of dielectric properties concerns storage and dissipation of electric and magnetic energy in materials. Dielectrics are important in order to explain various phenomena in Solid-State Physics and in Physics of Biological Materials.

Indeed, during the last two centuries, many scientists have tried to explain and model the dielectric relaxation. Starting from the Kohlrausch model and passing through the ideal Debye one, they arrived at more complex models that try to explain the experimentally observed distributions of relaxation times, including the classical (Cole-Cole, Davidson-Cole and Havriliak-Negami) and the more recent ones (Hilfer, Jonscher, Weron, etc.).

The purpose of this thesis is to discuss a variety of models carrying out the analysis both in the frequency and in the time domain. Particular attention is devoted to the three classical models, that are studied using a transcendental function known as Mittag-Leffler function. We highlight that one of the most important properties of this function, its complete monotonicity, is an essential property for the physical acceptability and realizability of the models.

Sommario

Lo studio delle proprietà dielettriche riguarda l'immagazzinamento e la dissipazione di energia elettrica e magnetica nei materiali. I dielettrici sono importanti al fine di spiegare vari fenomeni nell'ambito della Fisica dello Stato Solido e della Fisica dei Materiali Biologici.

Infatti, durante i due secoli passati, molti scienziati hanno tentato di spiegare e modellizzare il rilassamento dielettrico. A partire dal modello di Kohlrausch e passando attraverso quello ideale di Debye, sono giunti a modelli più complessi che tentano di spiegare la distribuzione osservata sperimentalmente di tempi di rilassamento, tra i quali modelli abbiamo quelli classici (Cole-Cole, Davidson-Cole e Havriliak-Negami) e quelli più recenti (Hilfer, Jonscher, Weron, etc.).

L'obiettivo di questa tesi è discutere vari modelli, conducendo l'analisi sia nel dominio delle frequenze sia in quello dei tempi. Particolare attenzione è rivolta ai tre modelli classici, i quali sono studiati utilizzando una funzione trascendente nota come funzione di Mittag-Leffler. Evidenziamo come una delle più importanti proprietà di questa funzione, la sua completa monotonia, è una proprietà essenziale per l'accettabilità fisica e la realizzabilità dei modelli.

Introduction

Dielectric properties of biological materials have been extensively studied since the second half of XIX century. To this topic has been attributed a rising attention during the decades; infact, in recent times, it was discovered that information about a body tissue structure and composition - water content or presence of a tumor, just to write an example - might be obtained by measuring the dielectric properties of the tissues. There is now the solid conviction that the understanding of interactions between electromagnetic energy and biological tissues must be based upon the knowledge of electrical properties of the materials; this leads to many practical appications in agriculture, food engineering and biomedical engineering.

However, going back to the beginning of the study of this topic, almost immediately quite a huge number of physicists and mathematicians began to investigate the frequency-dependent nature of the dielectric properties: they discovered that this behaviour may be described by relaxation processes associated with many physical materials displaying a time-dependent response to sudden excitation.

As it often occurs in Physics, the first approach was an idealized one: in order to find valid laws that described the frequency and time dependence of dielectric permettivity - to cite one of the most commonly studied dielectric properties - the system was reduced to its essential features, till a single charachteristic relaxation time was found. The description was so essential that this ideal behaviour, represented in Debye equation, can be found just in perfect liquids or in the case of almost perfect crystals. Anyway, the Debye

model, though it is not the first about dielectric investigation, has a very relevant role also in recent studies because it is considered to provide the first relaxation relationship derived on the basis of statistical mechanics and not just on the observation of experimental data.

Though the elegance of the Debye model formulation was evident, the data come from laboratories asked for some more attention: infact the dielectric properties of biological materials were complex and required a distribution of relaxation processes for their representation. This is the reason because of the birth of a wide variety of models that, using a distribution of relaxation times, provide formulas that try to fit the experimental data. This is the case, in particular, of the three classical models for anomalous relaxation: the Cole-Cole, the Davidson-Cole and the Havriliak-Negami that we will treat in our thesis.

Starting from the biophysical background behind the normal and the anomalous relaxation mechanisms, we will achieve a more rigorous and precise mathematical formalism of the three classical models; this treatise will involve the so called "Queen of fractional calculus", the Mittag-Leffler function, and the important mathematical-physical concept of complete monotonicity.

Outline

The outline of the thesis is the following.

In Chapter 1 we introduce the molecular origin of dielectric properties and the concept of pure Debye relaxation, indicating this simple model as the starting point for all the corrections and the other models.

In Chapter 2 we offer a review of the different models for anomalous relaxation; starting from the concept of multiple Debye process, we present the three classical models of Cole-Cole, Davidson-Cole and Havriliak-Negami, then we explain the Kohlrausch-Williams-Watts and the Hilfer models, finally arriving to the description of an attempt of universal law for dielectric relaxation and of the combined response model.

In Chapter 3 we introduce the Mittag-Leffler function in its version with one, two and three parameters and we give some mathematical description and details useful for the following chapter: we discuss the Laplace transforms of the Mittag-Leffler functions, their integral representations and asymptotic expansions, dedicating a section in particular to the complete monotonicity because this is what leads to the definition of the spectral density for the Mittag-Leffler.

In Chapter 4 we recall the three classical models presented in Chapter 2 but we discuss them in particular from the mathematical point of view because we explain that the models of Cole-Cole, Davidson-Cole and Havriliak-Negami can be considered insatnces of a general model described by a response function expressed in terms of the three-parameters Mittag-Leffler function. Great importance in this chapter is given to the graphics that show the behaviour of the relaxation function for the different models under exam, depending on the value of the parameters involved.

The mathematical details, for sake of clarity in the exposition of our thesis, have been written in four appendices: Appendix A and Appendix B are dedicated to two different proofs about the spectral density; Appendix C is a treatise of the properties of completely monotonic and Bernstein functions; Appendix D contains some details about the theory of entire functions, with particular attention to the Mittag-Leffler function, whose order and type are demonstrated.

Acknowledgements

I would like to take this opportunity to thank the various individuals to whom I am indebted, not only for their help in preparing this thesis, but also for their support and guidance through-out my studies.

I would first like to extend my thanks to my supervisor, Prof. Francesco Mainardi, for encouraging me to pursue this topic and for providing me all the advice and corrections I needed. Furthermore, I would like to thank my fellow students for their support and their feedback. Finally, I would like to thank those who have not directly been part of my academic life yet, but they have been of central importance in the rest of my life. First, and foremost, my parents, Silvia and Euro, for their continuous support and for teaching me the value of things. Also, to my brothers, Edoardo and Alessandro, who have had to deal with a sister often stressed by her work. I cannot forget my grandparents, Giancarlo, Liliana, Italo and Agnese, who have taught me - and they all continue to do it - the dedication, the sacrifice and the strenght of a resistent love. I also offer my thanks and apologies to my boyfriend, Luca, for having always patiently supported me though my frequent lack of self-convinction: you are as kind as you are pretious.

Ringraziamenti

Vorrei cogliere questa occasione per ringraziare le persone con cui sono in debito, non solamente per il loro aiuto nella preparazione di questa tesi, ma anche per il loro supporto e la loro guida nel corso dei miei studi.

Vorrei innanzitutto portare i miei ringraziamenti al mio supervisore, Prof. Francesco Mainardi, per avermi incoraggiato nell'affrontare questo argomento e per avermi fornito tutti i consigli e le correzioni di cui avevo bisogno. Inoltre, vorrei ringraziare i miei colleghi studenti per il loro supporto ed il loro riscontro. Infine, vorrei ringraziare coloro che non sono stati parte, per ora, della mia vita accademica, ma che hanno ricoperto un ruolo centrale nel resto della mia vita. Innanzitutto, e principalmente, i miei genitori, Silvia ed Euro, per il loro costante supporto e per avermi insegnato il valore delle cose. Poi, ai miei fratelli, Edoardo e Alessandro, che hanno dovuto avere a che fare con una sorella spesso agitata per il suo lavoro. Non posso dimenticare i miei nonni, Giancarlo, Liliana, Italo e Agnese, che mi hanno insegnato - e tutti loro continuano a farlo - la dedizione, il sacrificio e la forza di un amore tenace. Porgo i miei ringraziamenti e le mie scuse anche al mio fidanzato, Luca, per avermi sempre pazientemente supportato nonostante le mie frequenti carenze di fiducia in me stessa: sei gentile quanto prezioso.

Contents

List of Figures

Chapter 1

Biophysical background and Debye approach

All matter is constituted by charged entities held together by various atomic, molecular, and intermolecular forces. In this chapter we are going to analyse the effect of an externally applied electric field on the charge distribution, effect that is specific to the material under exam; the dielectric properties, infact, are a measure of that effect, being the intrinsic properties of matter used to characterize nonmetallic materials.

Biological matter has free and bound charges and, following the laws of classical electromagnetic theory, an applied electric field will cause them to drift and displace, inducing conduction and polarization currents. These mechanisms of polarization and conduction are the ones that underlie and explain the dielectric properties we are going to investigate. Because of the fact that dielectric phenomena and properties are indexed about the structure and composition of the material, their knowledge is of practical importance in all field of science where electromagnetic fields impinge on matter; for example this subject is of fundamental importance in electrophysiology, a branch of biomedical studies, in order to distinguish between the behaviour of various tissues, or in researches about the effect on biological material caused by the increasing of wireless telecommunication devices.

Though the electromagnetic field is what we study in general, we are in particular interested in its electric field component. Infact, for most biological materials, the magnetic permeability is close to that of free space - infact we say that the biological matter is diamagnetic - which implies that there is no direct interaction with the magnetic component of electromagnetic fields at low field strengths. However we have to say that there is a certain part of research about this subject that reports of the presence of magnetite in human nervous tissue, which suggest that magnetite may provide a mechanism for direct interaction of external magnetic fields with the human central nervous system. We are not treating this field of research in the present work because the role of these strongly magnetic materials in organisms is only just beginning to be unraveled.

1.1 Molecular origin of dielectric properties

Faraday was the first scientist who observed, in the 1830s, a change in the capacity of a capacitor when a dielectric was introduced inside it, with respect to the situation of empty capacitor. He found the well-known empirical formula for a capacitor filled with a dielectric:

$$C = \varepsilon C_0 = \varepsilon \frac{\varepsilon_0 A}{d}\,, \tag{1.1}$$

where ε is a dimensionless number that is the so called relative permettivity of the material and it is a fundamental properties of nonmetallic or dielectric materials being the ratio of the capacities of the filled and empty perfect capacitor of area A and plate separation d; ε_0 is the permettivity of free space and the product $\varepsilon\varepsilon_0$ is the absolute permettivity.

Since ε is a positive number, we have $C > C_0$ and this means an increase in capacity due to the addictional charge density induced in the material by the electric field that is said to have polarized the medium.

The polarization mechanism has three main components:

- the *electronic polarization* α_e is the shift of electrons in the direction

of the field from their equilibrium position with respect to the nuclei;

- the *atomic polarization* α_a is the relative displacement of atoms relative to each other;
- the *molecular polarization* α_m is the orientation of permanent or induced molecular dipoles and it is the most relevant contribution to the total polarization α_T.

When a dielectric becomes polarized by the application of a local electric field $\bar{E}_1$ acting on the molecules, the dipole moment of the constituent molecules is:

$$\bar{m} = \alpha_T \bar{E}_1 \,, \tag{1.2}$$

while the dipole moment per unit volume P increases the total displacement flux density D that becomes:

$$D = \varepsilon_0 E + P \,. \tag{1.3}$$

P depends on E and in the simplest case - for a perfect isotropic dielectric at low field intensisties and at static or quasi-static field frequencies - the proportionality between P and E is espressed through a scalar

$$\chi = \varepsilon - 1 \,, \tag{1.4}$$

the relative dielectric susceptibility:

$$P = \varepsilon_0 \chi E \,. \tag{1.5}$$

1.2 Time and frequency dependence of dielectric response

The dielectric properties are of high interest for the study of the response of biological materials to time-varying electric fields. Recalling (1.3) and introducing the time dependence of the field applied, the polarization mechanism is described by:

$$P(t) = D(t) - \epsilon_0 E(t) \,. \tag{1.6}$$

Thus, for an ideal dielectric material with no free charge, the polarization follows the pulse with a delay determined by the time constant τ of the polarization mechanism, according - in the simplest cases - to the formula:

$$P(t) = P(1 - e^{-t/\tau})\,. \tag{1.7}$$

For linear systems, the response to a unit-step electric field is the response function $f(t)$ of the siystem. The response of the system to a time-dependent field can be obtained from summation in a convolution integral of the impulses corresponding to a sequence of elements constituting the electric field. Considering a harmonic field and a causal, time-independent system, the Fourier transform exists and yelds, recalling (1.5):

$$P(\omega) = \epsilon_0 \chi(\omega) E(\omega)\,, \tag{1.8}$$

where the dielectric susceptibility $\chi(\omega)$ is the Fourier transform of $f(t)$.

In general $\chi(\omega)$ is a complex function

$$\chi(\omega) = \chi' - i\chi'' = \int_{-\infty}^{+\infty} \mathrm{e}^{i\omega t}\,\mathrm{d}t\,, \tag{1.9}$$

that informs on the magnitude and phase of the polarization with respect to the polarizing field. Its real and imaginary parts are obtained from the separate parts of the Fourier transform:

$$\chi'(\omega) = \int_{-\infty}^{+\infty} f(t)\,\cos(\omega t)\,dt = \int_{0}^{+\infty} f(t)\,\cos(\omega t)\,dt \tag{1.10a}$$

$$\chi''(\omega) = \int_{-\infty}^{+\infty} f(t)\,\sin(\omega t)\,dt = \int_{0}^{+\infty} f(t)\,\sin(\omega t)\,dt\,, \tag{1.10b}$$

where the lower limit of integration can be changed from $-\infty$ to 0 since $f(t)$ is a so-called causal function, meaning that it is a function of a single variable that is equal to zero if its variable is negative ($f(t) = 0$ if t$<$0).

The knowledge of the complex susceptibility $\chi(\omega)$ allows the detrmination of the impulse response $f(t)$ using the reverse Fourier transformation in order

to find $f(t)$ in terms of either $\chi'(\omega)$ or $\chi''(\omega)$:

$$f(t) = \frac{2}{\pi} \int_0^{+\infty} \chi'(\omega)\, \cos(\omega t)\, d\omega \tag{1.11a}$$

$$f(t) = \frac{2}{\pi} \int_0^{+\infty} \chi''(\omega)\, \cos(\omega t)\, d\omega\,. \tag{1.11b}$$

It is possible, eliminating $f(t)$ from the two relations above, to find two expressions that link the real and imaginary parts of the complex susceptibility - and consequently of the complex permettivity - of any material expressing them in terms of each other. These formulae are known as the Kramers-Krönig relations:

$$\chi'(\omega) = \chi'(\infty) + \frac{2}{\pi} \int_0^{+\infty} \frac{u\chi''(u) - \omega\chi''(\omega)}{u^2 - \omega^2}\, du \tag{1.12a}$$

$$\chi''(\omega) = \frac{2}{\pi} \int_0^{+\infty} \frac{u\chi'(u) - \chi'(\omega)}{u^2 - \omega^2}\, du\,. \tag{1.12b}$$

As mentioned above, since relative dielectric susceptibility χ and relative permittivity ε are related by $\chi = \varepsilon - 1$, also the permettivity is a complex function, with a real and an imaginary part, given by:

$$\hat{\varepsilon} = \varepsilon'(\omega) - i\varepsilon''(\omega) = [1 + \chi'(\omega)] - i[\chi''(\omega)]\,. \tag{1.13}$$

This notation for $\hat{\varepsilon}$ indicates the permettivity as the dielectric relaxation function of an ideal, noninteracting population of dipoles to an alternating external electric field.

1.3 Debye equation

When a step electric field E is applied to a polar dielectric material, the electronic and atomic polarization are established almost instantaneously compared to the time scale of the molecular orientation and polarization, and when that field is removed the process is reversed. The time constant τ that settles the delay in molecular polarization depends on the size, the shape and the intermolecular relations of the molecules.

In time varying fields we said that the permettivity is a complex function that takes origin from the magnitude and the phase shift of the polarization with respect to the polarizing field. Recalling (1.13) and defining the conductivity as:

$$\sigma = \omega\varepsilon_0\varepsilon'' \,, \tag{1.14}$$

we can write a new expression for the permittivity:

$$\hat{\varepsilon} = \varepsilon' - i\varepsilon'' = \varepsilon' - i\frac{\sigma}{\omega\varepsilon_0} \,, \tag{1.15}$$

where the real part is a measure of the induced polarization per unit field, while the imaginary part is the out-of-phase loss factor associated with it. The frequency response of the first-order system is obtained from the Laplace transformation, which provides the relationship known as the Debye equation:

$$\hat{\varepsilon} = \varepsilon_\infty + \frac{(\varepsilon_s - \varepsilon_\infty)}{1 + i\omega\tau} = \varepsilon' - i\varepsilon'' \,, \tag{1.16}$$

where ε_s and ε_∞ are the permettivities, respectively, at low and high frequency limit, while τ is the charachteristic relaxation time of the medium.

Equation (1.16) may be derived using a variety of microscopic models of the relaxation process. For example, Debye obtained it in 1929 by considering the rotational Brownian motion (excluding the inertial effects) of an assembly of electrically noninteracting dipoles.

The Debye equation can be transformed taking into account the conductivity $\hat{\sigma}$ instead of the permettivity $\hat{\varepsilon}$ giving:

$$\hat{\sigma} = \sigma_\infty + \frac{(\sigma_s - \sigma_\infty)}{1 + i\omega\tau} = \sigma' - i\sigma'' \,. \tag{1.17}$$

This model applies when one has a dilute solution of dipolar molecules in a nonpolar liquid, axially symmetric molecules and isotropy of the liquid, even on an atomic scale in the time average over a time interval which is small compared with the Debye relaxation time τ.

Dielectric relaxation phenomena had been extensively investigated long before the Debye relaxation law was proposed. For instance, Kohlrausch, in

1854, introduced the stretched exponential function (it is now also called the Kohlrausch function) to describe the charge relaxation phenomenon.

However, the Debye relaxation law might be the first relaxation relation derived on the bases of statistical mechanics; thus it has been often used, and we are going to consider it in the same way, as the starting point for investigating relaxation responses of dielectrics. The advantage of a formulation in terms of the Brownian motion is that the kinetic equations of that theory may be used to extend the Debye calculation to more complicated situations involving the inertial effects of the molecules and interactions between them. Moreover, the microscopic mechanisms underlying the Debye behaviour may be clearly understood in terms of the diffusion limit of a discrete time random walk on the surface of the unit sphere.

1.4 Conduction currents in Debye equation

In the previous section we had not taken into account the conduction mechanism whose effects are not included in pure Debye expression; the conduction, infact, is caused by the drift of free ions present in a non-ideal dielectric material, when exposed to static fields. If σ_s is the static conductivity, the Debye equation (1.16) gets an other term and becomes:

$$\begin{aligned}\hat{\varepsilon} &= \varepsilon_\infty + \frac{(\varepsilon_s - \varepsilon_\infty)}{1 - i\omega\tau} - \frac{i\sigma_s}{\omega\varepsilon_0} \\ &= \left[\varepsilon_\infty + \frac{(\varepsilon_s - \varepsilon_\infty)}{1 + (\omega\tau)^2}\right] - i\left[\frac{\sigma_s}{\omega\varepsilon_0} + \frac{(\varepsilon_s - \varepsilon_\infty)\omega\tau}{1 + (\omega\tau)^2}\right].\end{aligned} \tag{1.18}$$

The fact that the conductive term is negative means that this phenomenon is reducing the permettivity and the dielectric relaxation. Considering this addictional contribute to conduction, the total conductivity σ is given by:

$$\sigma = \omega\varepsilon_0\varepsilon'' = \sigma_s + \frac{(\varepsilon_s - \varepsilon_\infty)\varepsilon_0\omega^2\tau}{1 + (\omega\tau)^2}, \tag{1.19}$$

and, by this expression, we can note how the total conductivity is made of two terms corresponding to the residual static conductivity and polarization

losses; in practice it is only possible to measure the total conductivity of a material and, because of this, σ_s is obtained from data analysis or by measurement at frequencies corresponding to $\omega\tau \ll 1$, where the dipolar contribution to the total conductivity is neglegible.

Chapter 2

Models for anomalous relaxation

In the previous chapter we have described the expected behaviour of idealized biological materials but in practice very few materials exhibit a single relaxation time τ as in the Debye model: indeed greater or lesser changes are observed with respect to the ideal situation depending on the complexity of the underlying mechanisms. In order to describe these responses and to provide corrections to the Debye equation, the concepts of multiple dispersions and distribution of relaxation times have to be introduced.

Over the past 100 years, many empirical relaxation laws or relationships, which can be regarded as variants of the Debye relaxation law, have been developed, creating the theory of the so called anomalous relaxation. Among the most important are the Kohlrausch-Williams-Watts, the Cole-Cole, the Davidson-Cole and the Havriliak-Negami models, but we are presenting also a more recent one, the Hilfer model, particularly useful with certain experimental contexts. In practice, the empirical relationships provided by the different models work well for certain materials under specific conditions, but not for others.

Because of this experimental deviation of dielectric behaviour from what was expected according to the different models, in 1970s, Jonscher and his co-workers analyzed dielectric properties of many insulating and semiconducting materials; he then suggested that exists an universal law of dielectric

responses. Jonscher's work further stimulated scientific curiosity to explore the physical mechanism underlying the universal relaxation phenomenon. It is now well known that relaxation phenomena characterized by different physical quantities - and the permittivity is one of these - are very similar in different materials and most relaxation data can be interpreted by different types of experimental fitting functions.

2.1 Deviations from the Debye approach for dielectric relaxation

According to Debye relaxation process, all dipoles in the system relax with the same relaxation time (which is called a single relaxation time approximation) and the response function is purely exponential. Debye relaxation appears usually in liquids or in the case of point-defects of almost perfect crystals; but this pure Debye relaxation is very rare, therefore almost all real materials show non-Debye relaxation. This fact is due to the occurrence of multiple interaction processes, to the presence of more than one molecular conformational state or type of polar molecule, to polarization processes whose kinetics are not fist order or to the presence of complex intermolecular interactions.

Before starting the examination of the deviations from the Debye approach, we need to clarify the teminologies we are going to use and that in the common language could be erroneously confused as synonims: we are talking about the *relaxation* and *response* of the system under an electric strain. As pointed out by Karina Weron, the two terms are not equivalent and the reason regards the mathematical functions that are used to identify the behaviour of the system. What we call response function is properly the Laplace transform of the complex susceptibility that is different from the relaxation function. The relationship between the response function and the relaxation funtion can be better clarified by their probabilistic interpretation investigated for years by Weron. As a consequence, interpreting the relax-

ation function as a survival probability $\Psi(t)$, the response function turns out to be the probability density function corresponding to the cumulative probability function $\Phi(t) = 1 - \Psi(t)$. Then, denoting by $\phi(t)$ the response function, we have:

$$\phi(t) = -\frac{\mathrm{d}}{\mathrm{d}t}\Psi(t) = \frac{\mathrm{d}}{\mathrm{d}t}\Phi(t)\,, \qquad t \geq 0\,. \tag{2.1}$$

Both function have very different properties and describe different physical magnitudes and this is the reason that brought us to spend some words about. Only in the Debye case the properties of the functions coincide, while in general the relaxation function describes the decay of polarization whereas the response function its decay rate due to the depolarization currents. However, for physical realizability, we will see in the following chapters that both functions are required to be completely monotonic with a proper spectral density so our analysis can be properly transferred from response functions to the corresponding relaxation function, whereas the corresponding cumulative probability functions turn out to be Bernstein functions, that, like is diffusely explained in Appendix C, are positive functions with a completely monotonic derivative. In Chapters 3 and 4, it will appear evident our choice to denote the response function with $\xi(t)$ in order to be consistent with the notation $\widetilde{\xi}(s)$ for the complex susceptibility as a function of the frequency ω (since $s = i\omega$).

It is also important, before starting treating the three classical models, to highlight the proper difference between the different ways of studying the topic of the dielectric relaxation. Infact, there are three possible approaches to the topic: one based on frequencies, one on time and one on spectral densities.

As underlined by Hanyga, since experimental studies of dielectric relaxation are usually based on measurements of polarization of dielectric samples subject to periodic electric fields, a very common formulation in dielectric relaxation theory is frequency-domain based. Another approach is that time-domain based: it provides a more direct approach for the dielectric response to a suddenly applied electric field. Moreover, it is very useful

because frequency-domain formulation of material response is inappropriate in problems involving nonlinear expressions which are local in time. In particular, thermodynamic considerations involve bilinear expressions and therefore time-domain formulation of dielectric response is more convenient in this context. Last, but not least, time-domain formulation allows the use of powerful concepts and tools of harmonic analysis (non-negative definite functions, completely monotonic functions) and linear system theory. The third approach, based on the spectral densities, will be diffusely investigated in Chapter 3 and has two different formulation depending on the choice of a linear or a logarithmic scale.

Now, we are able to start examining the deviations from Debye relaxation, so introducing the anomalous one. The simplest case to deal with is the dielectric response arising from multiple first-order processes; it is quite easy to provide a correction to Debye equation since in this case the dielectric response consists of multiple Debye terms, one for each relaxation time of the system:

$$\hat{\varepsilon} = \varepsilon_\infty + \frac{\Delta\varepsilon_1}{1 - i\omega\tau_1} + \frac{\Delta\varepsilon_2}{1 - i\omega\tau_2} + \dots , \tag{2.2}$$

where $\Delta\varepsilon_n$ is the limit of the dispersion charachterized by time constant τ_n. If the relaxation times are well separated such that $\tau_1 \ll \tau_2 \ll \tau_3 \ll ...$, a plot of the dielectric properties as a function of frequency wll exhibit clearly resolved dispersion regions. Conversely, if the relaxation times are not well separated, the material will exhibit a broad dispersion encompassing all the relaxation times and the dispersion regions mentioned above become, in the limit, part of a continuous distribution of relaxation times. The Debye equation is thus modified reaching the following expression:

$$\hat{\varepsilon} = \varepsilon_\infty + (\varepsilon_s - \varepsilon_\infty) \int_0^\infty \frac{\rho(\tau)\, d\tau}{1 - i\omega\tau} , \tag{2.3}$$

where $\rho(\tau)$ is a normalized distibution function:

$$\int_0^\infty \rho(\tau)\, d\tau = 1 . \tag{2.4}$$

According to (2.3), it would be possible to represent all dielectric dispersion data, once an appropriate distribution function is provided and known; by

the other side, it should also be possible to invert diectric relaxation spectra to determine $\rho(\tau)$ directly. Anyway, this second option is not of practical use because of the difficulty in inverting the spectra but, more commonly, one has to assume a distribution to describe the frequency dependence of the dielectric properties observed experimentally. The choice of distribution function should depend on the cause of the multiple dipersions in the material. For example, one can assume a Gaussian distribution with τ as the mean relaxation time:

$$\rho(t/\tau) = \frac{b}{\sqrt{\pi}} e^{-(t/\tau - b)^2} . \tag{2.5}$$

As it is shown in Figure 2.1, the shape of the Gaussian function depends on the parameter b: it reduces to the delta function when b tends to infinity and becomes very broad when b decreases. The problem of Gaussian distribution is that, if we incorporate this ρ into the expression for complex permettivity $\hat{\varepsilon}$, the expression produced cannot be solved analytically and it is useless in experimental data analysis.

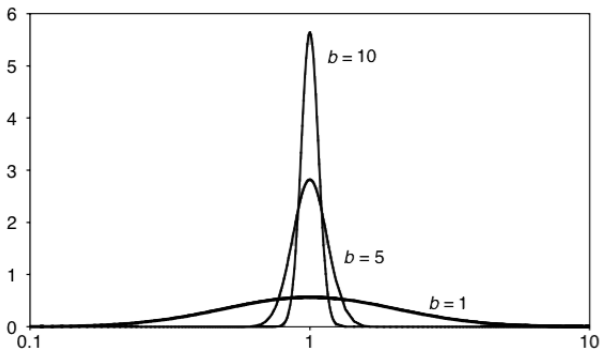

Figure 2.1: Gaussian distribution function as a function of t/τ in logarithmic scale.

Thus, the topic of this chapter has become finding an empirical distribution function or model in order to fit the experimental data. We are going to start explaining three different models that begin from Debye equation and then modify its expression: these are Cole-Cole, Davidson-Cole and Havriliak-Negami models.

2.2 Cole-Cole model

One of the most commonly used models was proposed in 1941 by Cole and Cole and is widely known as the Cole-Cole model:

$$\hat{\varepsilon}_{CC} = \varepsilon_\infty + \frac{(\varepsilon_s - \varepsilon_\infty)}{1 - (i\omega\tau)^\alpha} = \varepsilon'_{CC} - i\varepsilon''_{CC}\,. \tag{2.6}$$

In this expression, α is a distribution parameter in the range $0 < \alpha \leq 1$. Comparing (2.6) with (1.16), it is clear that for $\alpha = 1$, the Cole-Cole model reverts to Debye equation. The real and imaginary parts of the complex permettivity are:

$$\varepsilon'_{CC} = \varepsilon_\infty + \frac{(\varepsilon_s - \varepsilon_\infty)[1 - (\omega\tau)^\alpha \cos(\alpha\pi/2)]}{1 + (\omega\tau)^{2\alpha} + 2(\omega\tau)^\alpha \cos(\alpha\pi/2)} \tag{2.7a}$$

$$\varepsilon''_{CC} = -\frac{(\varepsilon_s - \varepsilon_\infty)(\omega\tau)^\alpha \sin(\alpha\pi/2)}{1 + (\omega\tau)^{2\alpha} + 2(\omega\tau)^\alpha \cos(\alpha\pi/2)}\,. \tag{2.7b}$$

Eliminating $\omega\tau$ from the above equations can be found the following equation:

$$\left(\varepsilon'_{CC} - \frac{(\varepsilon_s + \varepsilon_\infty)}{2}\right)^2 + \left(\varepsilon''_{CC} + \frac{(\varepsilon_s + \varepsilon_\infty)}{2}\cot\frac{\alpha\pi}{2}\right)^2 = \left(\frac{(\varepsilon_s - \varepsilon_\infty)}{2}\operatorname{cosec}\frac{\alpha\pi}{2}\right)^2, \tag{2.8}$$

that indicates that the plot of ε'_{CC} against ε''_{CC} is a semicircle with its center below the real axis, while the Debye equivalent of the equation above would be:

$$\left(\varepsilon' - \frac{(\varepsilon_s + \varepsilon_\infty)}{2}\right)^2 + \varepsilon''^2 = \left(\frac{\varepsilon_s - \varepsilon_\infty}{2}\right)^2, \tag{2.9}$$

which indicates that a plot of ε' against ε'' is a semicircle with its centre exactly on the real axis. The mentioned plots, called *Cole-Cole plots* or *Cole-Coles*, can be found in Chapter 4, where we are going to analyse all the graphics about the classical models for dielectric relaxation, more precisely in Figure 4.1.

The distribution function that corresponds to the Cole-Cole model is:

$$\rho_{CC}(t/\tau) = -\frac{1}{2\pi}\frac{\sin(\alpha\pi)}{\cosh[\alpha \ln(t/\tau)] + \cos(\alpha\pi)}\,, \tag{2.10}$$

where τ is the mean relaxation time. As with the Gaussian, we can see in Figure 2.2 that this distribution is logarithmically symmetrical about t/τ.

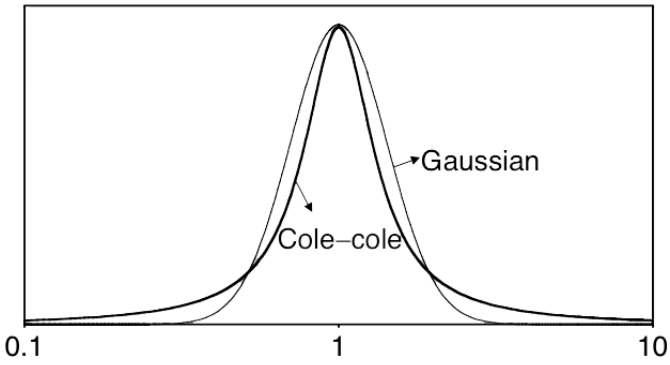

Figure 2.2: Gaussian distribution with $b = 2$ and Cole-Cole distribution with $\alpha = 0.01$ as a function of t/τ in logarithmic scale.

2.3 Davidson-Cole model

In 1951, Davidson and Cole, after having studied the behaviour of a particular group of polar liquids that didn't correspond to the Cole-Cole model, proposed another variant of the Debye equation in which an exponent γ is applied to the whole denominator:

$$\hat{\varepsilon}_{DC} = \varepsilon_\infty + \frac{(\varepsilon_s - \varepsilon_\infty)}{(1 - i\omega\tau)^\gamma} = \varepsilon'_{DC} - i\varepsilon''_{DC}\,. \tag{2.11}$$

In this expression, γ is a distribution parameter in the range $0 < \gamma \leq 1$. Comparing (2.11) with (1.16), it is clear that for $\gamma = 1$, the Davidson-Cole model reverts to Debye equation. The real and imaginary parts of the complex permettivity are:

$$\varepsilon'_{DC} = \varepsilon_\infty + (\varepsilon_s - \varepsilon_\infty)\cos(\gamma\phi)(\cos\phi)^\gamma \tag{2.12a}$$

$$\varepsilon''_{DC} = (\varepsilon_s - \varepsilon_\infty)\sin(\gamma\phi)(\cos\phi)^\gamma\,, \tag{2.12b}$$

where

$$\phi = \arctan(\omega\tau)\,. \tag{2.13}$$

The Cole-Cole plot for Davidson-Cole model - so, the plot of the real and imaginary parts of the model - presents, as it will be shown in Figure 4.3, a skewed arc, similar to the Debye plot at low frequencies, but different at high frequencies.

The distribution function that corresponds to the Davidson-Cole model is:

$$\rho_{DC}(t/\tau) = \frac{1}{\pi}\left(\frac{t}{\tau - t}\right)^{\gamma} \sin(\pi\gamma)\,, \tag{2.14}$$

and it is shown graphically in Figure 2.3, exhibiting a singularity at $t/\tau = 1$, while it returns zero at $t < \tau$.

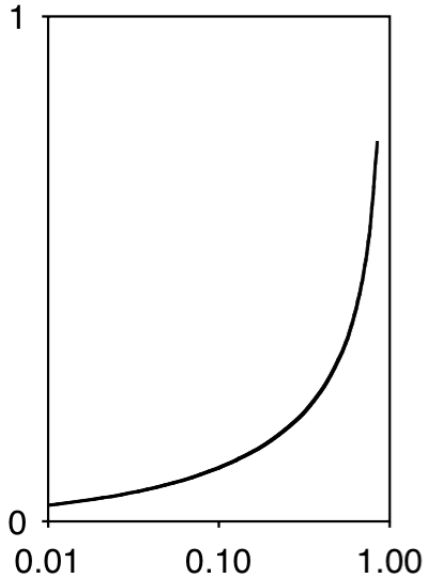

Figure 2.3: Davidson-Cole distribution with $\gamma = 0.5$ as a function of t/τ in logarithmic scale.

2.4 Havriliak-Negami model

Another expression, sometimes used to model dielectric data, is that proposed by Havriliak and Negami in 1966. In order to describe the anomalous (according to Cole-Cole and Davidson-Cole models) data of experiments conduced by the two scientists on policarbonates, the model combines the variations introduced in both the Cole-Cole and the Davidson-Cole models, giving:

$$\hat{\varepsilon}_{HN} = \varepsilon_{\infty} + \frac{(\varepsilon_s - \varepsilon_{\infty})}{(1 - (i\omega\tau)^{\alpha})^{\gamma}} = \varepsilon'_{HN} - i\varepsilon''_{HN}\,. \tag{2.15}$$

Comparing (2.15) with (1.16), (2.6) and (2.11), it is clear that Havriliak-Negami expression reverts to its Cole-Cole, Davidson-Cole and Debye equivalents at the limiting values of $\gamma = 1$, $\alpha = 1$ and $\alpha = 1$ and $\gamma = 1$, respectively. The real and imaginary parts of the complex permettivity are:

$$\varepsilon'_{HN} = \varepsilon_\infty + \frac{(\varepsilon_s - \varepsilon_\infty)\cos(\gamma\phi)}{1 + 2(\omega\tau)^\alpha \cos(\alpha\pi/2) + (\omega\tau)^{(2\alpha)^{\gamma/2}}} \tag{2.16a}$$

$$\varepsilon'_{HN} = \frac{(\varepsilon_s - \varepsilon_\infty)\sin(\gamma\phi)}{1 + 2(\omega\tau)^\alpha \cos(\alpha\pi/2) + (\omega\tau)^{(2\alpha)^{\gamma/2}}}\,, \tag{2.16b}$$

where

$$\phi = \arctan \frac{-(\omega\tau)^\alpha \sin(\alpha\pi/2)}{1 + (\omega\tau)^\alpha \cos(\alpha\pi/2)}\,. \tag{2.17}$$

The Cole-Cole plot of the Havriliak-Negami model is an asymmetric curve intercepting the real axis at different angles at high and low frequencies, as it will be shown in Figure 4.5.

The distribution function that corresponds to the Havriliak-Negami model is:

$$\rho_{HN}(t/\tau) = \frac{1}{\pi} \frac{(t/\tau)^{\gamma\alpha}\sin(\gamma\theta)}{(t/\tau)^{2\alpha} + 2(t/\tau)^\alpha \cos(\alpha\pi) + 1)^{\gamma/2}}\,, \tag{2.18}$$

where

$$\theta = \arctan \frac{\sin(\alpha\pi)}{(t/\tau) + \cos(\alpha\pi)}\,. \tag{2.19}$$

Like the Cole-Cole plot for this model, that is an asymmetric curve, also the distribution of relaxation times is asymmetric, as shown in Figure 2.4.

All the models presented in this section provide empirical distribution functions without giving any mechanistic justification; however, the Debye model and its many variations have been widely used over more than half a century primarily because they lend themselves to simple curve-fitting procedures. In particular, the Cole-Cole model is used almost as a matter of course in the analysis of the dielectric properties of biological materials.

2.5 Kohlrausch-Williams-Watts model

Mathematically, at the limit of high frequencies, the Cole-Cole function simplifies to a fractional power law since both ε' and ε'' are proportional to

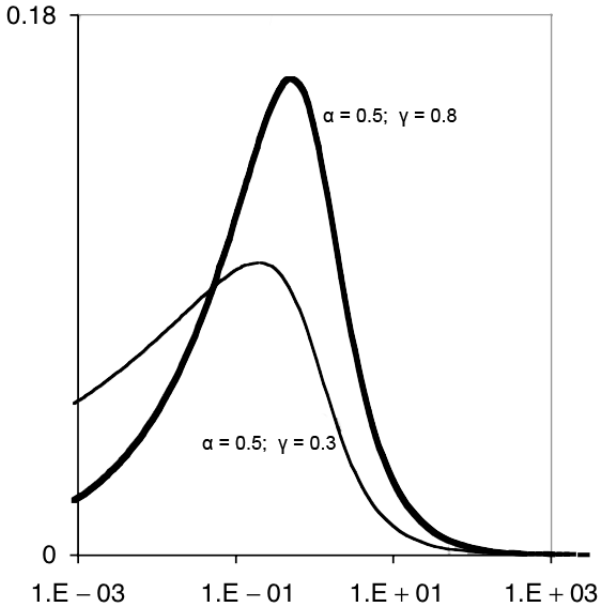

Figure 2.4: Havriliak-Negami distribution as a function of t/τ in logarithmic scale, showing the effect of γ for a given value of α.

$(\omega\tau)^{\alpha}$. This fractional power law behaviour is at the basis of what is known as the universal law of dielectric phenomena developed by Jonsher, Hill and Dissado for the analysis of the frequency dependence of dielectric data.

An other fractional power law was also inserted in the exponential function by Kohlrausch in 1854, while he was studying a way to describe the process of discharge of a capacitor; but, in a certain sense, the same function was "redescovered" more then a century later, in 1970, by Williams and Watts who used the Fourier transform of the stretched exponential to describe dielectric spectra of polymers. These contributions of these three scientists designed a new model for dielectric relaxation: it was born the Kohlraush-Williams-Watts model.

The model we are going to present is based on the *stretched exponential function* that is also the response function of this model:

$$f_{\beta}(t) = e^{-(t/\tau_{\beta})^{\beta}}, \tag{2.20}$$

where the exponent is $0 < \beta \leq 1$ and τ_{β} is a time constant. The name

attributed to the function above is due to the fact that it is obtained by inserting a fractional power law into the exponential function; for $\beta = 1$, the usual exponential function is recovered while with a stretching exponent β between 0 and 1, the graph of ln $f_\beta(t)$ versus t is characteristically stretched, hence the name of the function. The compressed exponential function with $\beta > 1$ has less practical importance, with the notable exception of the case $\beta = 2$ which gives the normal distribution.

As mentioned above, in Physics the stretched exponential function is often used as a phenomenological description of relaxation in disordered systems. It was first introduced by Rudolf Kohlrausch in 1854 in order to describe the discharge of a capacitor and, because of this, the function in (2.20) is also known as the Kohlrausch function. More then a century later, precisely in 1970, Graham Williams and David Watts used the Fourier transform of the stretched exponential to describe dielectric spectra of polymers: in this context, the stretched exponential or its Fourier transform are also called the Kohlrausch-Williams-Watts (KWW) function.

Differently from the Cole-Cole, Davidson-Cole and Havriliak-Negami models, the Kohlrausch-Williams-Watts model is a model in the domain of time and not in that of frequency. Anyway it is possible to transfer the KWW function in the domain through the formula:

$$\widehat{\chi}(\omega) = 1 + i\omega\widetilde{f}(s)\,, \tag{2.21}$$

where $\widetilde{f}(s)$ is the Laplace transform of the relaxation function $f(t)$.

Using (2.21) and applying it to (2.20) we obtain for the susceptibility the result:

$$\widehat{\chi}_{KWW}(\omega) = \widehat{\varepsilon}_{KWW}(\omega) - 1 = 1 - \sum_{n=0}^{\infty} \frac{\Gamma(\beta n + 1)}{\Gamma(n+1)} \left(-(-i\omega\tau_\beta)^\beta\right)^{-n}\,, \tag{2.22}$$

where the series is convergent for all $0 < |(-i\omega\tau_\beta)^\beta| < \infty$.

The success of Kohlrausch-Williams-Watts model is due to the fact that various authors observed that stretched exponential functions are often more appropriate in modelling relaxation processes in bone, muscles, dielectric

materials, polymers and glasses than standard exponentials of Debye-type. In part, this is a consequence of the fact that, because a relaxation depends on the entire spectrum of relaxation times, its structure will be non-linear and not purely exponential.

2.6 Hilfer model

Amorphous polymers and supercooled liquids near the glass transition temperature exhibit strongly nonexponential response and relaxation functions in various experiments. Infact, dielectric spectroscopy experiments show an asymmetrically broadened relaxation peak, often called the α-relaxation peak, that flattens into an excess wing at high frequencies.

Most theoretical and experimental works use a small number of empirical expressions such as the Cole-Davidson, Haviriliak-Negami or Kohlrausch-Williams-Watts formulae for fitting the asymmetric α-relaxation peak (the Cole-Cole model is excluded because it gives a symmetric peak). All of these phenomenological fitting formulae are obtained by the method of introducing a fractional stretching exponent into the standard Debye relaxation in the time or frequency domain.

Hilfer, starting from the three models seen and described above, introduces in four works a simple 3-parameters fit function that works well not only for fitting the asymmetric α-peak, but also for the excess wing at high frequencies. The functional form is:

$$\widehat{\chi}_H(\omega) = \frac{1 + (-i\omega\tau_\alpha)^\alpha}{1 + (-i\omega\tau_\alpha)^\alpha - i\omega\tau'_\alpha}\,, \tag{2.23}$$

containing a single stretching exponent $0 < \alpha \leq 1$ and two relaxation times $\tau_\alpha > 0$ and $\tau'_\alpha < \infty$.

The functional form was obtained by Hilfer studying the theory of fractional dynamics, a matter we are not intended to investigate in the present context. Rather, it is interesting to compare the new function with the traditional functions at the level of a phenomenological fitting function. The

results are presented for the broadband dielectric spectra of glass-forming propylene carbonated and reported in an experimental work of Schneider, Lunkenheimer, Brand and Loidl [Schneider, Brand et al. 2000]. At a temperature of $T = 193$ K the dielectric spectrum shows a broadened α-peak and excess high-frequency wing over roughly five decades in frequency. The data are then fitted separately for the real and imaginary part. The fit uses only data from three decades (from $f = 10^{5.1}$ to $10^{8.1}$ Hz) around the maximum of the imaginary part as indicated by vertical dashed lines in the figure.

The two-step Debye fit uses:

$$\widehat{\chi}(\omega) = \frac{1 - i\omega\tau_2(1-C)}{(1-i\omega\tau_1)(1-i\omega\tau_2)}\,, \tag{2.24}$$

where $0 < \tau_1 < \tau_2 < \infty$ are the two relaxation times and C is a parameter that fixes the relative dielectric strenght of the two relaxation processes.

The Davidson-Cole fit uses:

$$\widehat{\chi}(\omega) = \frac{1}{(1-i\omega\tau_\gamma)^\gamma}\,, \tag{2.25}$$

where $0 < \gamma \leq 1$.

The Havriliak-Negami fit uses:

$$\widehat{\chi}(\omega) = \frac{1}{(1+(-i\omega\tau_H)^{\alpha\gamma}}\,, \tag{2.26}$$

where there are two stretching exponents $\alpha > 0$ and $\gamma \leq 1$ and one relaxation time $0 < \tau_H < \infty$.

The Kohlrausch-Williams-Watts fit uses:

$$\widehat{\chi}(\omega) = 1 - \sum_{n=0}^{\infty} \frac{\Gamma(\beta n + 1}{\Gamma(n+1)} \left(-(-i\omega\tau_\beta)^\beta\right)^{-n}\,, \tag{2.27}$$

where the stretching exponent is $0 < \beta \leq 1$ and τ_β is a time constant.

Finally, the Hilfer fit uses (2.23).

In all fits an additional fit is the isothermal susceptibility $\phi(0) = \chi_0 - \chi_\infty$ where χ_0 is the static susceptibility ($\chi_0 = \lim_{\omega\to 0} \mathrm{Re}\chi(\omega)$) while χ_∞ gives the instantaneous response ($\chi_\infty = \lim_{\omega\to\infty} \mathrm{Re}\chi(\omega)$).

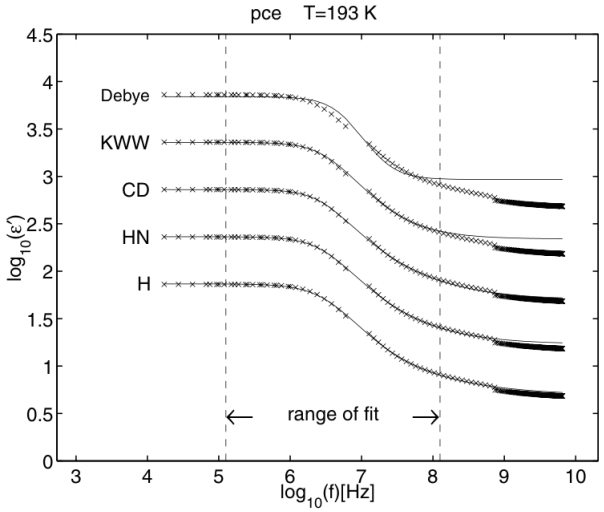

Figure 2.5: Five different fits to the real part $\varepsilon'(\omega) = \mathrm{Re}\chi(\omega)$ of the complex dielectric function of propylene carbonate at $T = 193$K as a function of frequency. The original location of the data corresponds to the curve labelled H.

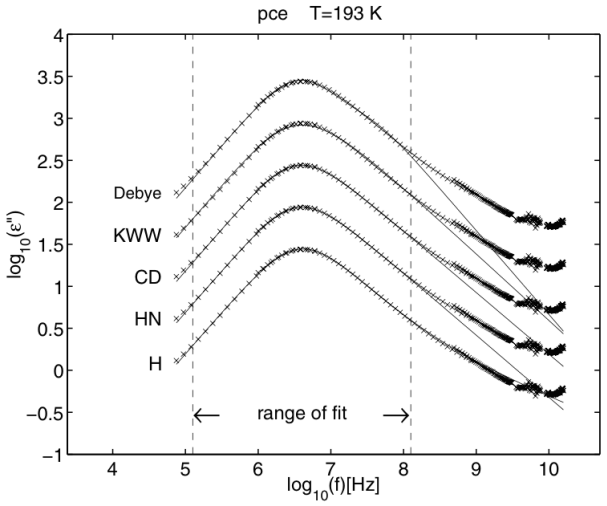

Figure 2.6: Five different fits to the imaginary part $\varepsilon''(\omega) = \mathrm{Im}\chi(\omega)$ of the complex dielectric function of propylene carbonate at $T = 193$K as a function of frequency. The original location of the data corresponds to the curve labelled H.

Figure 2.5 shows the results for the real part. The data have been displaced in the vertical direction from their original location corresponding to the Hilfer fit, in order to show more clarly the quality of the different fits. Clearly the two-step Debye fit in not as good as the other fits in the fitting range. Extending the fitting range shows also that the Kohlrausch-Williams-Watts formula does not give as good an agreement as the Davidson-Cole, Havriliak-Negami and Hilfer ones. This can also be seen from the fact that the latter fits extend beyond the original fitting range.

Otherwise, Figure 2.6 shows the results for the imaginary part. They deviate significantly from the experimental data in the excess wing region outside the fitting range. Extending the fit range for the Davidson-Cole and Havriliak-Negami fits would give poorer agreement and systematic deviations around the main peak.

In contrast to the Davidson-Cole and Havriliak-Negami fits, the Hilfer one extends well beyond the fitting range into the region of the excess wing. Extending the fit range in this case would not lower the quality of the fit near the main peak. This makes the Hilfer model an excellent one because a simple functional form, with only a single stretching exponent, allows one to fit an asymmetrically broadened relaxation peak well into the excess wing.

2.7 Universal law of dielectric relaxation

Jonscher and his collaborators collated and analyzed extensive dielectric data obtained from numerous sources, pertaining to a wide range of materials, measured over a broad range of temperatures and frequencies. Their aim was to observe how dielectrics behave rather than presume a model for their frequency dependence; they studied the data on a logaritmic scale to better recognize the presence of a power law dependence, if present.

Very few materials exhibit a pure Debye behavior where, at frequencies in excess of ω_p, the logarithmic slopes for $\varepsilon'(\omega)$ and $\varepsilon''(\omega)$ are -2 and -1, respectively, which is a Kramers-Krönig compatible result. However, for most

materials a power law dependence of the type ω^{n-1}, with $n \neq 0$, applies for both $\varepsilon'(\omega)$ and $\varepsilon''(\omega)$. This is in compliance with the Kramers-Krönig relations, which require that at frequencies exceeding ω_p, both parameters follow the same frequency dependence, making the ratio $\frac{\varepsilon''(\omega)}{\varepsilon''(\omega)}$ frequency independent. Under such conditions, the ratio of energy dissipated to energy stored per radian of sinusoidal excitation is constant. The universal law can be summarized by the following frequency dependencies for the normalized complex permittivity:

$$\text{for} \quad \omega < \omega_p\,, \qquad \varepsilon''(\omega) \approx \omega^m \qquad \text{and} \qquad \varepsilon'(\omega) \approx 1 - \varepsilon''(\omega)\,, \tag{2.28}$$

$$\text{for} \quad \omega > \omega_p\,, \qquad \varepsilon''(\omega) \approx \omega^{n-1} \qquad \text{and} \qquad \varepsilon'(\omega) \approx \varepsilon''(\omega) \approx \omega^{n-1}\,. \tag{2.29}$$

Observation of the experimental data showed that ω_p is temperature T dependent and follows an Arrhenius function:

$$\omega_p = Ae^{-W/kT} \tag{2.30}$$

and the functional form for $\varepsilon''(\omega)$ is:

$$\varepsilon''(\omega) = \frac{A}{\left(\frac{\omega}{\omega_p}\right)^{1-n} + \left(\frac{\omega_p}{\omega}\right)^m}\,. \tag{2.31}$$

The values for $\varepsilon'(\omega)$ can then be determined numerically from the Kramer-Krönig relations.

Although the features of the dielectric spectra of most maerials can be described using this approach, ther is no theoretical justification for it. This makes it yet another empirical model, albeit a very general and mathematically elegant one.

2.8 Combined response model

A model that combines features from Debye-type and universl dielectric response behaviour was proposed by Raicu in 1999 in [Raicu 1999]. Trying to

find a model of broad dielectric dispensions, as is often observed in the dielectric spectrum of biological materials, Raicu found that neither approach was good enough over a wide frequency range. He proposed the following very general function for the complex permettivity:

$$\hat{\varepsilon}_R = \varepsilon_\infty + \frac{\Delta}{[(i\omega\tau)^\alpha + (i\omega\tau)^{1-\beta}]^\gamma} \tag{2.32}$$

where α, β and γ are real constants in the range [0,1], τ is the charachteristic relaxation time and Δ is a dimensional constant which becomes the dielectric increment $(\varepsilon_s - \varepsilon_\infty)$ when $\alpha = 0$. The above expression reverts to Havriliak-Negami model (2.15) - which further reduces to the Debye (1.16), Cole-Cole (2.6) or Davidson-Cole (2.11) models - with an appropriate choice of the α, β and γ. For $\gamma = 1$, it reverts to Jonsher's universal response law; in the special case where $\gamma = 1$ and $\alpha = 1 - \beta$, it becomes:

$$\hat{\varepsilon}_R = \varepsilon_\infty + \left(i\frac{\omega}{s}\right)^{\beta-1} \tag{2.33}$$

which is known as the constant phase angle model. In this expression s is a scaling factor given by $s = (\Delta/2)^{1/(1-\beta)}\tau^{-1}$. The abocve expression was successfully used to model the dielectric spectrum of a biological material over five frequency decades from 10^3Hz to 10^8Hz.

A proper study of dielectric properties of biological materials starts from here. The purpose is to study the properties of a tissue, a complex and heterogenous material containing water, dissolved organic molecules, macromolecules, ions and insoluble matter; the constituents are themselves highly organized in cellular and subcellular structures forming macroscopic elements and soft and hard tissues; the presence of ions plays an important role in the interaction with an electric field, providing means for ionic conduction and polarization effects; ionic charge drift creates conduction currents and also initiates polarization mechanisms through charge accumulation at structural interfaces, which occur at various organizational levels. Because of all these complex contributions, the dielectric properties of tissue will reflect the different components of polarization given from both structure and composition.

A more precise study of this topic would begin here: the contribution of each of the components (water, carbohydrates, proteins, other macromolecules, electrolytes) has to be determined individually and then collectively, leading to the formulation of models for the dielectric response of biological tissue.

Chapter 3

Mittag-Leffler functions

After having described, in Chapter 2, the expressions for the three classical models for dielectric relaxation, the purpose of this third chapter is to introduce the study of the so-called "Queen function of fractional calculus" - the Mittag-Leffler function in its version with one, two and three parameters - in order to show, in Chapter 4, that the three classical models already presented (Cole-Cole, Davidson-Cole and Havriliak-Negami) can be considered instances of a general model described by a response function expressed in terms of the three-parameters Mittag-Leffler function.

The Mittag-Leffler type functions are so named after the great Swedish mathematician Gösta Mittag-Leffler who introduced and investigated them at the beginning of the 20-th century, in a sequence of five works. Even though these functions have been ignored for long time to the majority of scientists, since the times of their father several physicists and mathematicians recognized their importance, providing interesting mathematical and physical applications. For example, in mathematical field was found the solution of the Abel integral equation of the second kind in terms of a Mittag-Leffler function and other types of Mittag-Leffler functions were used to express the general soluton of the linear fractional differential equation with constant coefficients. Concerning the physical field, there were important contributions about nerve conduction, viscoelastic models and mechanical and dielectric

relaxation.

3.1 Definitions and properties

3.1.1 1-parameter Mittag-Leffler function

The Mittag-Leffler function $E_\alpha(z)$ is defined by the following series representation, which is valid in the whole complex plane,

$$E_\alpha(z) := \sum_0^\infty \frac{z^n}{\Gamma(\alpha n + 1)}\,, \tag{3.1}$$

where $\alpha > 0$ is a real parameter and z is the complex variable. It turns out that $E_\alpha(z)$ is an entire function - it means that it is a complex-valued function that is holomorphic over the whole complex plane - of order $\rho = 1/\alpha$ and type 1. This property remains still valid but with $\rho = 1/\mathrm{Re}\{\alpha\}$, in $\alpha \in \mathbb{C}$ with positive real part. A deeper treatment of entire functions can be found in Appendix D.

Under the limit $\alpha \longrightarrow 0^+$ the function loses the analicity in the whole complex plane, since

$$E_0(z) = \sum_0^\infty z^n = \frac{1}{1-z}\,, \quad |z| < 1\,, \tag{3.2}$$

due to the presence of a simple pole in $z = 1$.

Notable cases are:

$$E_2(+z^2) = \cosh z\,, \qquad E_2(-z^2) = \cos z\,, \qquad z \in \mathbb{C}\,, \tag{3.3}$$

from which elementary hyperbolic and trigonometric functions are recovered, and

$$E_{1/2}(\pm z^{1/2}) = \mathrm{e}^z\left[1 + \mathrm{erf}\left(\pm z^{1/2}\right)\right] = \mathrm{e}^z \mathrm{erfc}\left(\mp z^{1/2}\right)\,, \qquad z \in \mathbb{C}\,. \tag{3.4}$$

where $\mathrm{erf}(z)$ denotes the so called error function, and $\mathrm{erfc}(z)$ denotes its complementary, defined as

$$\mathrm{erf}(z) = \frac{2}{\sqrt{\pi}} \int_0^z \mathrm{e}^{-u^2} du\,, \quad \mathrm{erfc}(z) = 1 - \mathrm{erf}(z)\,, \quad z \in \mathbb{C}\,. \tag{3.5}$$

3.1.2 2-parameters Mittag-Leffler function

A logical generalization of the Mittag-Leffler function is obtained by substituting the additive constant 1 in the argument of the Gamma function in (3.1) with an arbitrary complex parameter β, namely:

$$E_{\alpha,\beta}(z) := \sum_{0}^{\infty} \frac{z^n}{\Gamma(\alpha n + \beta)}\,, \tag{3.6}$$

where α is the scalar already met in the definition of 1-parameter Mittag-Leffler function.

Two notable examples of this two-indexes function have to be mentioned:

$$E_{1,2}(z) = \frac{\mathrm{e}^z - 1}{z}\,, \quad E_{2,2}(z) = \frac{\sinh(z^{1/2})}{z^{1/2}}\,. \tag{3.7}$$

3.1.3 3-parameters Mittag-Leffler function

One more step can be done introducing a third complex index γ, so defining the 3-parameter Mittag-Leffler function, known as Prabhakar function too:

$$E^{\gamma}_{\alpha,\beta}(z) := \sum_{n=0}^{\infty} \frac{(\gamma)_n}{n!\Gamma(\alpha n + \beta)}\, z^n\,, \tag{3.8}$$

where α, β and γ are complex numbers with the condition that $\mathrm{Re}\{\alpha\} > 0$ and where

$$(\gamma)_n = \gamma(\gamma+1)\ldots(\gamma+n-1) = \frac{\Gamma(\gamma+n)}{\Gamma(\gamma)} \tag{3.9}$$

are called Pochhammer symbols and they are defined for every $n \in \mathbb{N}$.

Also the 3-parameters Mittag-Leffler is an entire function of order $\rho = 1/\mathrm{Re}\{\alpha\}$, and for $\gamma = 1$ we recover the 2-parameter Mittag-Leffler function $E^1_{\alpha,\beta}(z) = E_{\alpha,\beta}(z)$ as well as for $\gamma = \beta = 1$ we recover the standard 1-parameter Mittag-Leffler function $E^1_{\alpha,1}(z) = E_{\alpha}(z)$.

3.2 The Laplace transform pairs related to the Mittag-Leffler functions

Let us now consider the relevant formulas of Laplace transform pairs related to the above three functions already known in the literature when the independent variable is real of type at where $t > 0$ may be interpreted as time and a as a certain constant of frequency dimensions. For the sake of convenience we adopt the notation $\div$ to denote the juxtaposition of a function of time $f(t)$ with its Laplace transform $\widetilde{f}(s) = \int_0^\infty \mathrm{e}^{-st} f(t)\, dt$. So, introducing the notation used by Capelas de Oliveira in which $e^{\gamma}_{\alpha,\beta}(t) =: t^{\beta-1} E^{\gamma}_{\alpha,\beta}(-t^{\alpha})$, we have:

$$e_{\alpha}(t;-a) := E_{\alpha}(at^{\alpha}) \;\div\; \frac{s^{-1}}{1-as^{-\alpha}} = \frac{s^{\alpha-1}}{s^{\alpha}-a}\,, \tag{3.10}$$

$$e_{\alpha,\beta}(t;-a) := t^{\beta-1}\, E_{\alpha,\beta}(at^{\alpha}) \;\div\; \frac{s^{-\beta}}{1-as^{-\alpha}} = \frac{s^{\alpha-\beta}}{s^{\alpha}-a}\,, \tag{3.11}$$

$$e^{\gamma}_{\alpha,\beta}(t;-a) := t^{\beta-1}\, E^{\gamma}_{\alpha,\beta}(at^{\alpha}) \;\div\; \frac{s^{-\beta}}{(1-as^{-\alpha})^{\gamma}} = \frac{s^{\alpha\gamma-\beta}}{(s^{\alpha}-a)^{\gamma}}\,. \tag{3.12}$$

In general, with five positive arbitrary parameters $\alpha, \beta, \gamma, \delta, \rho$ the function $t^{\rho-1}\, E^{\gamma}_{\alpha,\beta}(at^{\delta})$ has a Laplace transform expressed in terms of a transcendental function of Wright hypergeometric type. Therefore, it is possible to link these two famous functions. A celebrated case, which will be focused in the rest of this chapter, is obtained for the constant $a = -1$.

3.3 Integral representation and asymptotic expansions

Many relevant properties of the Mittag-Leffler class of functions $E_{\alpha}(z)$ follow from its integral representation:

$$E_{\alpha}(z) = \frac{1}{2\pi i} \int_{Ha} \frac{\zeta^{\alpha-1}\, e^{\zeta}}{\zeta^{\alpha}-z}\, d\zeta\,. \tag{3.13}$$

Here, the path of integration Ha indicates the so-called Hankel's path, a contour which, starting from and ending at $-\infty$, encircles the circular disk

$|\zeta| \leq |z|^{\alpha}$ in the positive sense ($-\pi \leq \arg(\zeta) \leq \pi$). This proof can be given by expanding the integrand in powers of ζ, integrating term-by-term and using the Hankel's integral for the reciprocal of the Gamma function. The integrand in (3.13) has a branch-point at $\zeta = 0$. A cut along the negative real axis is operated in order to obtain a single-valued integrand: the principal branch of ζ^{α} is taken in the cut plane. The integrand has also poles at $\zeta_m = z^{1/\alpha} e^{2\pi i m/\alpha}$ with $m \in \mathbb{Z}$, but only the poles for which $-\alpha\pi < \arg(z) + 2\pi m < \alpha\pi$ lie in the cut plane. Thus, the number of poles inside the Hankel's path is either α or $\alpha + 1$, according to the value of $\arg(z)$.

The integral representation of the 2-parameters Mittag-Leffler function is:

$$E_{\alpha,\beta}(z) = \frac{1}{2\pi i} \int_{Ha} \frac{\zeta^{\alpha-\beta}\ e^{\zeta}}{\zeta^{\alpha} - z} d\zeta\,. \tag{3.14}$$

Of particular interest are the properties of the Mittag-Leffler functions associated with its asymptotic behavior for $|z| \to \infty$. For the case $0 < \alpha < 2$ the limit depends on the sector of the complex plane in which the limit is studied:

$$\begin{aligned} E_{\alpha}(z) &\sim \frac{1}{\alpha}\exp(z^{1/\alpha}) - \sum_{1=n}^{\infty} \frac{z^{-n}}{\Gamma(1-\alpha n)}, \qquad |z| \to \infty, \qquad |\arg(z)| < \alpha\pi/2 \\ E_{\alpha}(z) &\sim -\sum_{1=n}^{\infty} \frac{z^{-n}}{\Gamma(1-\alpha n)}, \qquad |z| \to \infty, \qquad \alpha\pi/2 < \arg(z) < 2\pi - \alpha\pi/2. \end{aligned} \tag{3.15}$$

For the case $\alpha \geq 2$:

$$E_{\alpha}(z) \sim \frac{1}{\alpha} \sum_{m} \exp(z^{1/\alpha}\ e^{2\pi i m/\alpha}) - \sum_{1=n}^{\infty} \frac{z^{-n}}{\Gamma(1-\alpha n)}, \qquad |z| \to \infty, \tag{3.16}$$

where m takes all integer values such that $-\alpha\pi/2 < \arg(z) + 2\pi m < \alpha\pi/2$ and $|z| \leq \pi$.

3.4 Complete monotonicity

Though a more complete and deeper analysis of complete monotonic function is provided in Appendix C, let us recall that a real non-negative function

$f(t)$ defined for $t \in \mathbb{R}^+$ is said to be completely monotonic if it possesses derivatives $f^{(n)}(t)$ for all $n = 0, 1, 2, 3, ...$ that are alternating in sign:

$$(-1)^n f^{(n)}(t) \geq 0 \qquad t > 0\,. \tag{3.17}$$

The limit $f^{(n)}(0^+) = \lim_{t\to 0^+} f^{(n)}(t)$ finite or infinite exists. From the Bernstein theorem it is known that a necessary and sufficient condition for having $f(t)$ completely monotonic is that

$$f(t) = \int_0^\infty e^{-rt}\, d\mu(r)\,, \tag{3.18}$$

where $\mu(r)$ is a non-decreasing function and the integral converges for $0 < t < \infty$. In other words, $f(t)$ is required to be expressed as the real Laplace Transform of a non-negative function in particular:

$$f(t) = \int_0^\infty e^{-rt} K(r)\, dr\,, \tag{3.19}$$

where $K(r) \geq 0$ is the standard or generalized function known as kernel or, better, spectral density.

This is a crucial point of our analysis because a process, governed by the function $f(t)$ with $f \geq 0$, can be expressed in terms of a continuous distribution of elementary (exponential) relaxation processes with frequencies r on the whole range $]0, \infty[$.

Moreover, as discussed by several authors, the complete monotonicity is an essential property for the physical acceptability and realizability of the models since it ensures, for instance, that in isolated systems the energy decays monotonically as expected from physical considerations. Studying the conditions under which the response function of a system in completely monotonic is therefore of fundamental importance.

The property because of that the energy of a system decays monotonically is called *weak dissipativity* and it ensures that every energy compatible with the constitutive equation does not exceed its original value immediately after the system was displaced from equilibrium. For viscoelastic systems, weak dissipativity is satisfied by the non-convex relaxation modulus $G(t)$.

Unless the relaxation modulus G is either completely monotonic or convex and integrable, it is not known whether the system has a strongly dissipative energy bounded from below. Strongly dissipative energies exist in some special classes of systems and one of them in the class of viscoelastic systems with completely monotonic relaxation. A strongly dissipative energy associated with a system is not unique. A conserved energy can be constructed for a large class of weakly dissipative systems with locally integrable relaxation moduli. A conjecture, not already demonstrated, is that for a completely monotonic system the energy has the highest dissipation rate.

The latter considerations are explained by Hanyga about viscoelastic systems but corresponding considerations can be done about dielectric ones because of the electromechanic analogy between the two systems.

In the case of the pure exponential $f(t) = \exp(-\lambda t)$ with a given relaxation frequency $\lambda > 0$ we have $K(r;\lambda) = \delta(r - \lambda)$.

Since $\widetilde{f}(s)$ is the Laplace transform of $f(t)$ and this one, in turn, is the Laplace transform of $K(r)$, $\widetilde{f}(s)$ becomes the iterated Laplace transform of $K(r)$; so, we can recognize that $\widetilde{f}(s)$ is the Stieltjes transform of $K(r)$

$$\widetilde{f}(s) = \int_0^\infty \frac{K(r)}{s+r}\,\mathrm{d}r\,, \tag{3.20}$$

and therefore the spectral density $K(r)$ can be determined as the inverse Stieltjes transform of $\widetilde{f}(s)$ via the Titchmarsh inversion formula proved in [Titchmarsh 1937], finding:

$$K(r) = \mp\frac{1}{\pi}\,\mathrm{Im}[\widetilde{f}(s)|_{s=re^{\pm i\pi}}]\,. \tag{3.21}$$

3.4.1 $K_{\alpha,\beta}(r)$: spectral density of 2-parameters Mittag-Leffler

The results written in this section until this point are valid in general for completely monotonic function such as $f(t)$. Now, we want to apply them to the object of our analysis: the Mittag-Leffler functions. For the Mittag-Leffler functions in one and two-order parameter the conditions to be completely

monotonic on the negative real axis were found by Capelas de Olieveira, Mainardi and Vaz and are respectively $0 < \alpha \leq 1$ in the first case and $0 < \alpha \leq 1\,,\ \beta \geq \alpha$ in the second. We assume $a = -1$, because the function at^α must be negative, so the corresponding Laplace transform pair in (3.11) becomes:

$$e_{\alpha,\beta}(t, -(-1)) = t^{\beta-1}\, E_{\alpha,\beta}(-t^\alpha) \ \div\ \frac{s^{-\beta}}{1+s^{-\alpha}} = \frac{s^{\alpha-\beta}}{s^\alpha+1}\,. \tag{3.22}$$

We prove the existence of the corresponding spectral density using the complex Bromwich formula to invert the Laplace transform. Taking $0 < \alpha < 1$ the denominator does not exhibit any zero so, bending the Bromwich path into the equivalent Hankel path mentioned above, we get:

$$e_{\alpha,\beta}(t, +1) = t^{\beta-1}\, E_{\alpha,\beta}(-t^\alpha) = \int_0^\infty e^{-rt}\, K_{\alpha,\beta}(r)\, \mathrm{d}r\,, \tag{3.23}$$

with

$$K_{\alpha,\beta}(r) = -\frac{1}{\pi}\,\mathrm{Im}\left[\frac{s^{\alpha-\beta}}{s^\alpha+1}|_{s=re^{i\pi}}\right] = \frac{r^{\alpha-\beta}}{\pi}\,\frac{\sin[(\beta-\alpha)\pi] + r^\alpha \sin(\beta\pi)}{r^{2\alpha} + 2r^\alpha\cos(\alpha\pi) + 1}\,. \tag{3.24}$$

We easily recognize

$$K_{\alpha,\beta}(r) \geq 0 \quad \text{if} \quad 0 < \alpha \leq \beta \leq 1\,, \tag{3.25}$$

including the limiting case $\alpha = \beta = 1$ where Mittag-Leffler function reduces to the exponential $\exp(-t)$ and $K_{1,1}(r) = \delta(r-1)$. Infact, the denominator in (3.24) is non negative being greater or equal to $(r^\alpha - 1)^2$ and the numerator is non negative as soon as the two sin functions are both non-negative. We note that the conditions (3.25) on the parameters α and β can also be justified by noting that in this case the resulting function is completely monotonic as a product of two completely monotonic functions. In fact $t^{\beta-1}$ is completely monotonic if $\beta < 1$ whereas $E_{\alpha,\beta}(-t^\alpha)$ is completely monotonic if $0 < \alpha \leq 1$ and $\beta \geq \alpha$.

The behaviour of the spectral densities for the 2-parameters Mittag-Leffler function, for different values of α can be seen in graphics in Figures 3.1, 3.2, 3.3 and 3.4.

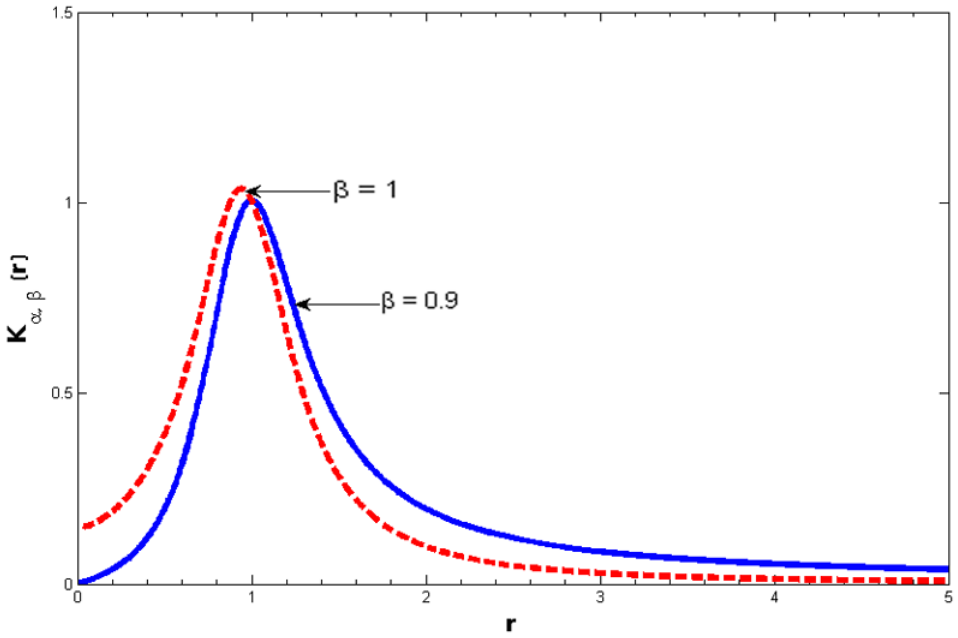

Figure 3.1: 2-parameters spectral density $K_{\alpha,\beta}(r)$ calculated for $\alpha = 0.9$

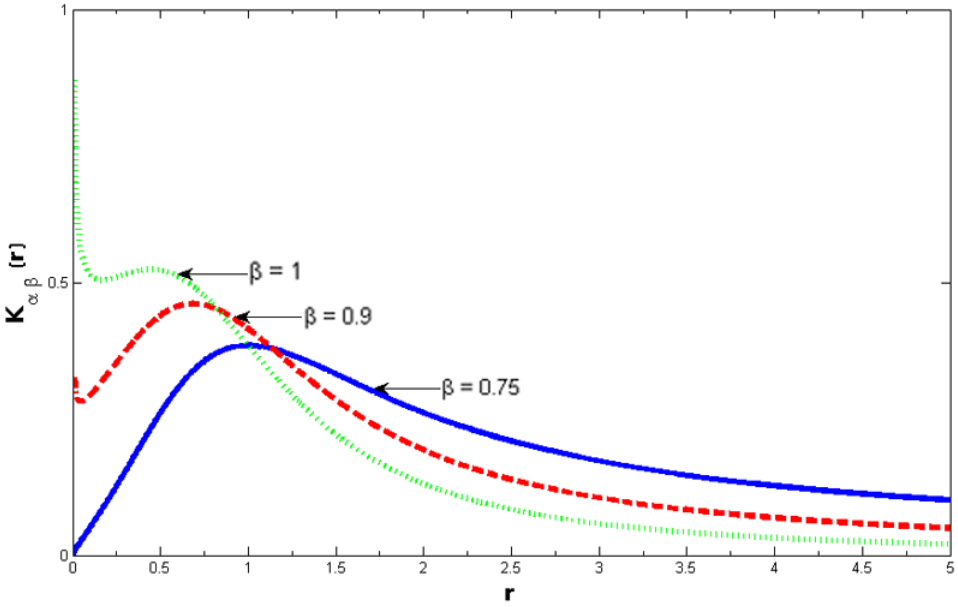

Figure 3.2: 2-parameters spectral density $K_{\alpha,\beta}(r)$ calculated for $\alpha = 0.75$

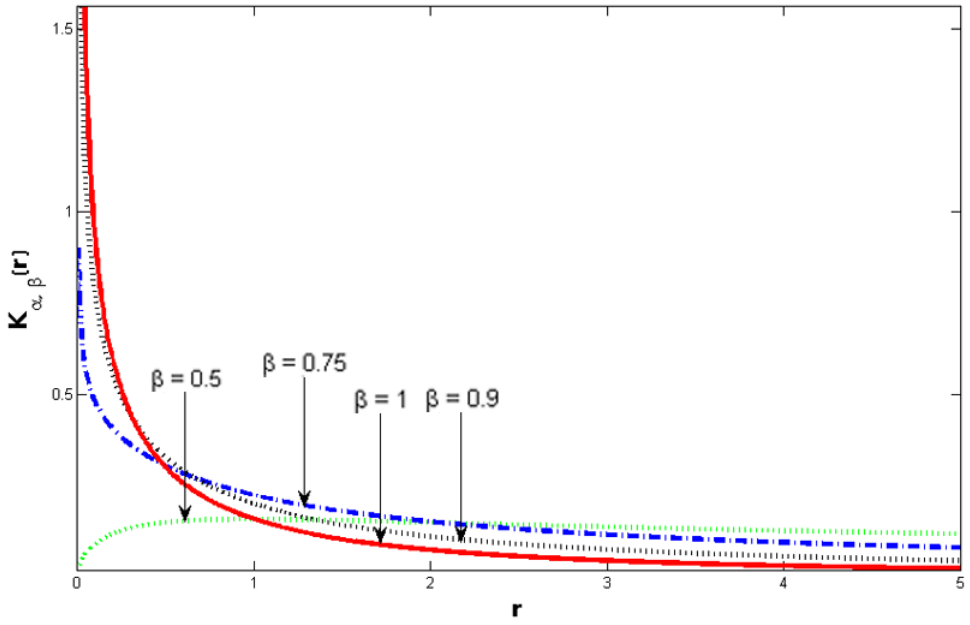

Figure 3.3: 2-parameters spectral density $K_{\alpha,\beta}(r)$ calculated for $\alpha = 0.5$

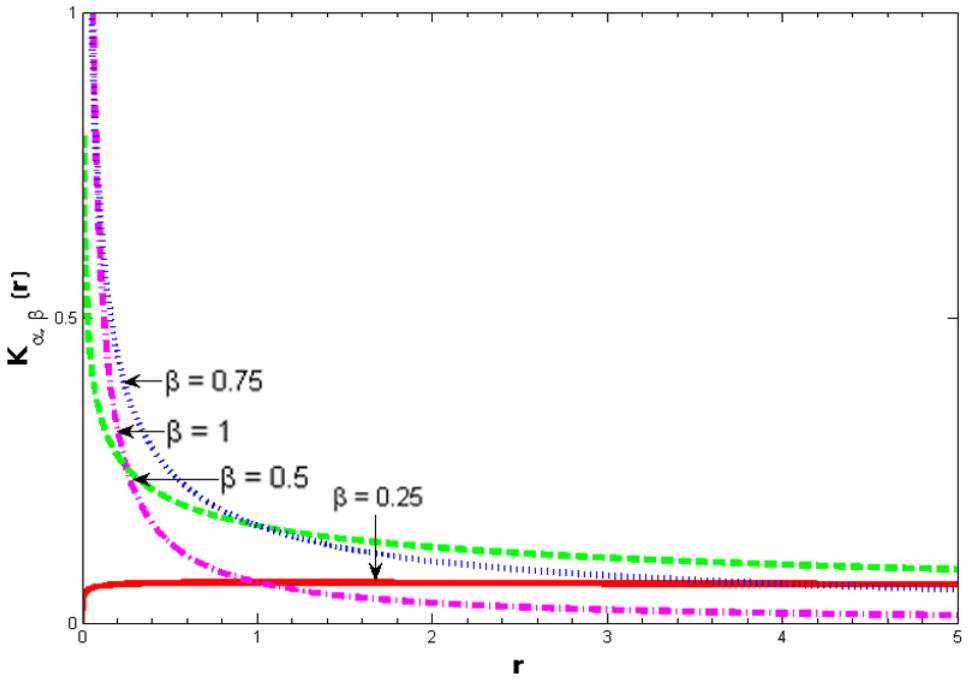

Figure 3.4: 2-parameters spectral density $K_{\alpha,\beta}(r)$ calculated for $\alpha = 0.25$

3.4.2 $K_\alpha(r)$: spectral density of 1-parameter Mittag-Leffler

The spectral density for the standard Mittag-Leffler function with only one parameter is found in the particular case in which $\beta = 1$ and we have the following two expressions:

$$e_\alpha(t, +1) = E_\alpha(-t^\alpha) = \int_0^\infty e^{-rt}\, K_\alpha(r)\, \mathrm{d}r\,, \tag{3.26}$$

$$K_\alpha(r) = \frac{r^{\alpha-1}}{\pi}\, \frac{\sin(\alpha\pi)}{r^{2\alpha} + 2r^\alpha \cos(\alpha\pi) + 1}\,. \tag{3.27}$$

The graphic behaviour of $K_\alpha(r)$ for four different values of α can be seen in Figures 3.1, 3.2, 3.3 and 3.4, paying attention to focus on the plots with $\beta = 1$ since $K_\alpha(r)$ is properly $K_{\alpha,1}(r)$.

3.4.3 $K^\gamma_{\alpha,\beta}(r)$: spectral density of 3-parameters Mittag-Leffler

After having described the expressions and showed the behaviour of the spectral density for 1 and 2-parameters Mittag-Leffler functions, an analysis of the more general 3-parameters function has to be done.

Recalling (3.12) we define, for $a = -1$, the following function:

$$\xi_G(t) := t^{\beta-1}\, E^\gamma_{\alpha,\beta}(-t^\alpha)\,, \tag{3.28}$$

G meaning general, because in next section we are going to apply this line of reasoning to the models for dielectric relaxation. Always according to (3.12), we can write the Laplace transform of $\xi_G(t)$:

$$\widetilde{\xi}_G(s) = \frac{s^{-\beta}}{1 + s^{-\alpha}} = \frac{s^{\alpha\gamma-\beta}}{(s^\alpha + 1)^\gamma}\,. \tag{3.29}$$

In analogy with the previous computing for 2-parameters Mittag-Leffler, we get:

$$\xi_G(t) = \int_0^\infty e^{-rt}\, K^\gamma_{\alpha,\beta}(r)\, \mathrm{d}r\,, \tag{3.30}$$

with the spectral density

$$K^{\gamma}_{\alpha,\beta}(r) = \frac{1}{\pi} \frac{r^{\alpha\gamma-\beta}}{\left(r^{2\alpha} + 2r^{\alpha}\,\cos(\alpha\pi) + 1\right)^{\frac{\gamma}{2}}} \sin\left[\gamma \arctan\left(\frac{r^{\alpha}\sin(\pi\alpha)}{r^{\alpha}\cos(\pi\alpha)+1}\right) + (\beta - \alpha\gamma)\pi\right]. \tag{3.31}$$

A formal demonstration of this spectral density starts from the application of the Titchmarsh formula (3.21). The complete proof of the above result is written in Appendix A, while in Appendix B is shown how, for $\gamma = 1$ the above expression reduces to (3.24), the spectral density of the 2-parameters Mittag-Leffler function.

In exposing the theory of spectral density we wanted $K(r) \geq 0$ and this often happens under certain conditions. Concerning to the case we are studying, the conditions on the parameters α, β and γ required to ensure the non negativity of the spectral density (3.31) consist in the following inequalities that can be written in two equivalent forms and that are proved in Appendix C using the Gripenberg theorem:

$$0 < \alpha \leq 1\,, 0 < \beta \leq 1,\ 0 < \gamma \leq \frac{\beta}{\alpha} \Longleftrightarrow 0 < \alpha \leq 1\,, 0 < \alpha\gamma \leq \beta \leq 1 \tag{3.32}$$

that for $\gamma = 1$ reduce to the single inequality $0 < \alpha \leq \beta \leq 1$ that coincides with the condition required for the two-parameter Mittag-Leffler function in (3.25).

If $\alpha\gamma = \beta$, (3.31) reduce to a spectral density which depends by two only parameters:

$$K^{\gamma}_{\alpha,\alpha\gamma}(r) = \frac{1}{\pi} \frac{1}{\left(r^{2\alpha} + 2r^{\alpha}\,\cos(\alpha\pi) + 1\right)^{\frac{\gamma}{2}}} \sin\left[\gamma \arctan\left(\frac{r^{\alpha}\sin(\pi\alpha)}{r^{\alpha}\cos(\pi\alpha)+1}\right)\right]. \tag{3.33}$$

Since the spectral density $K^{\gamma}_{\alpha,\beta}(r)$ must not be negative and since the first two factors are certainly positive, the argument of trigonometric function sin has to be in $[0, \pi]$; but now we note that the definition of $\arctan x$, as function into $\left(-\frac{\pi}{2}, \frac{\pi}{2}\right)$, is not well-defined to our purpose, and to avoid negative values we need to add π. So, calling for brevity χ the argument of the arctangent:

$$\chi = \frac{r^{\alpha}\sin(\pi\alpha)}{r^{\alpha}\cos(\pi\alpha)+1}\,, \tag{3.34}$$

we can write:

$$\theta = \begin{cases} \arctan(\chi) & \chi > 0\,, \\ \arctan(\chi) + \pi & \chi < 0\,. \end{cases} \tag{3.35}$$

Chapter 4

Mathematical analysis of classical models

In the present chapter we want to use the results given in Chapter 3 in order to apply them to the description of the mathematical models for the response function and the complex susceptibility in the framework of a general relaxation theory of dielectrics.

In Chapter 2 we showed the expressions for complex permettivity according to the three classical models of Cole-Cole, Davidson-Cole and Havriliak-Negami: now we want to demonstrate that all these models are contained in a general model described by a response function expressed in terms of the 3-parameters Mittag-Leffler function under the condition $\alpha\gamma - \beta = 0$, according to the following scheme:

$$\begin{cases} 0 < \alpha < 1\,, \beta = \alpha\,, \gamma = 1 & \text{Cole-Cole } \{\alpha\}\,, \\ \alpha = 1\,, \beta = \gamma\,, 0 < \gamma < 1 & \text{Davidson-Cole } \{\gamma\}\,, \\ 0 < \alpha < 1\,, 0 < \gamma < 1 & \text{Havriliak-Negami } \{\alpha, \gamma\}\,. \end{cases} \tag{4.1}$$

It is of some interest to notice that all the expressions in the scheme above satisfy the condition $\alpha\gamma - \beta = 0$.

Later in this chapter we are going to consider some more general cases when the equality $\alpha\gamma - \beta = 0$ is not satisfied while the inequality $0 < \alpha\gamma \leq \beta$ holds provided $0 < \alpha \leq 1$, $0 < \beta \leq 1$, in agreement with (3.32).

4.1 Cole-Cole mathematical model

Let us recall that the Cole-Cole (C-C) relaxation model is a non-Debye relaxation model depending on one parameter $\alpha \in]0,1[$, that reduces to the standard Debye model for $\alpha = 1$.

According to the correspondent condition in (4.1) and taking into account (3.28), we have to refer to the following response function:

$$\xi_{\text{C-C}}(t) = t^{\alpha-1}\, E^1_{\alpha,\alpha}(-t^\alpha) \tag{4.2}$$

and, according to (3.29), to its Laplace transform:

$$\widetilde{\xi}_{\text{C-C}}(s) = \frac{1}{1+s^\alpha}\,. \tag{4.3}$$

It is not difficult to compare (4.3) with (2.6) and to find the same structure for the complex permettivity with the suitable change of variable.

The Cole-Cole plot for this model, according to (2.8), is shown in Figure 4.1 and the apexes of the arcs correspond to the mean relaxation frequency. It is important to recall that when $\alpha = 1$ the Cole-Cole reverts to Debye model and also in the Cole-Cole plots this is true and shown: infact, while the plot of ε'_{CC} against ε''_{CC} is a semicircle with its center below the real axis, in the limit in which α becomes 1, the plot of ε' agains ε'' shows the center of the semicircle exactly on the real axis, according to (2.9).

The spectral density for the Cole-Cole model is easily obtained from (3.31):

$$K_{\text{C-C}}(r) = K^1_{\alpha,\alpha}(r) = \frac{1}{\pi}\,\frac{r^\alpha \sin(\alpha\pi)}{r^{2\alpha} + 2r^\alpha \cos(\alpha\pi) + 1}\,. \tag{4.4}$$

The graphic in Figure 4.2 shows the behaviour of $K_{\text{C-C}}(r)$ for different values of the parameter α.

Noting that $K_{\text{C-C}}(r)\Big|_{r\longrightarrow\infty} \sim \frac{1}{r^\alpha}$, running so to zero, it is easy to find its maximum value in $r = 1$:

$$K_{\text{C-C}}(r=1) = \frac{1}{2\pi}\frac{\sin\alpha\pi}{\cos\alpha\pi + 1} = \frac{1}{2\pi}\tan\frac{\alpha\pi}{2}\,. \tag{4.5}$$

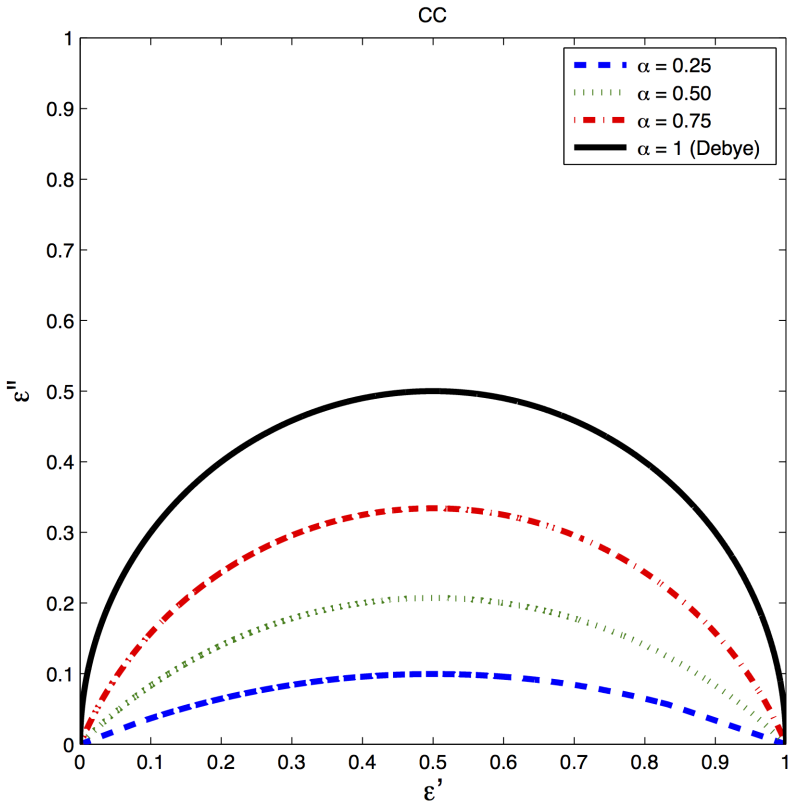

Figure 4.1: Plot of normalized permettivity $\frac{(\varepsilon'-\varepsilon_\infty)}{(\varepsilon_s-\varepsilon_\infty)}$ against loss factor $\frac{\varepsilon''}{(\varepsilon_s-\varepsilon_\infty)}$ showing a semicircle with his center on real axis in the case of the Debye and an arc of a semicircle with its center below the real axis in the case of the Cole-Cole, for various values of the parameter α.

4.2 Davidson-Cole mathematical model

The Davidson-Cole (D-C) relaxation model is a non-Debye relaxation model depending on one parameter $\gamma \in]0,1[$, that reduces to the standard Debye model for $\gamma = 1$.

According to the correspondent condition in (4.1) and taking into account (3.28), we have to refer to the following response function:

$$\xi_{\text{D-C}}(t) = t^{\gamma-1}\, E^{\gamma}_{1,\gamma}(-t) \tag{4.6}$$

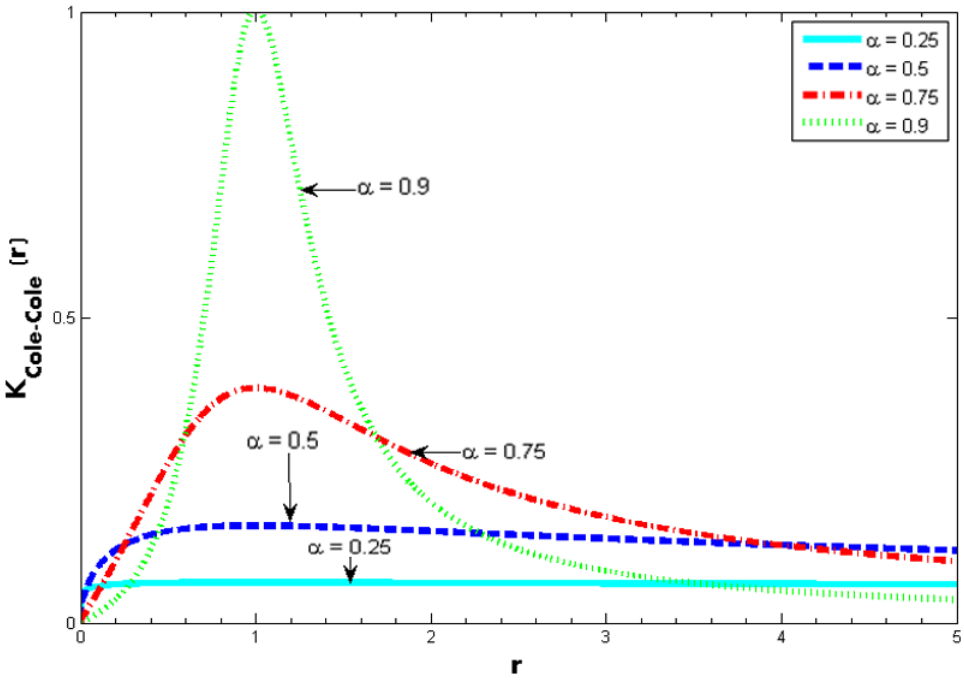

Figure 4.2: The spectral density for the Cole-Cole model $K_{\text{C-C}}(r) := K^1_{\alpha,\alpha}(r)$ calculated for $\alpha = 0.9$, $\alpha = 0.75$, $\alpha = 0.5$ and $\alpha = 0.25$.

and, according to (3.29), to its Laplace transform:

$$\widetilde{\xi}_{\text{D-C}}(s) = \frac{1}{(1+s)^{\gamma}}\,. \tag{4.7}$$

Comparing (4.7) with (2.11), it is easy to find the same structure for the complex permettivity with the suitable change of variable.

In Figure 4.3 is shown the Cole-Cole plots, the plots of the real and imaginary parts of the complex permettivity for different values of γ, for this model, according to (2.12a). It is easy to notice that the plots present a skewed arc, similar to the Debye plot at low frequency but deviating from it at high frequency.

The spectral density for the Cole-Cole model is easily obtained noticing that the response function $\xi_{\text{D-C}}(r)$ is the Laplace transform of itself, so that:

$$K_{\text{D-C}}(r) := K^{\gamma}_{1,\gamma}(r) = \begin{cases} 0 & 0 < r < 1\,, \\ (r-1)^{-\gamma}\,\frac{\sin\gamma\pi)}{\pi} & r > 1\,, \end{cases} \tag{4.8}$$

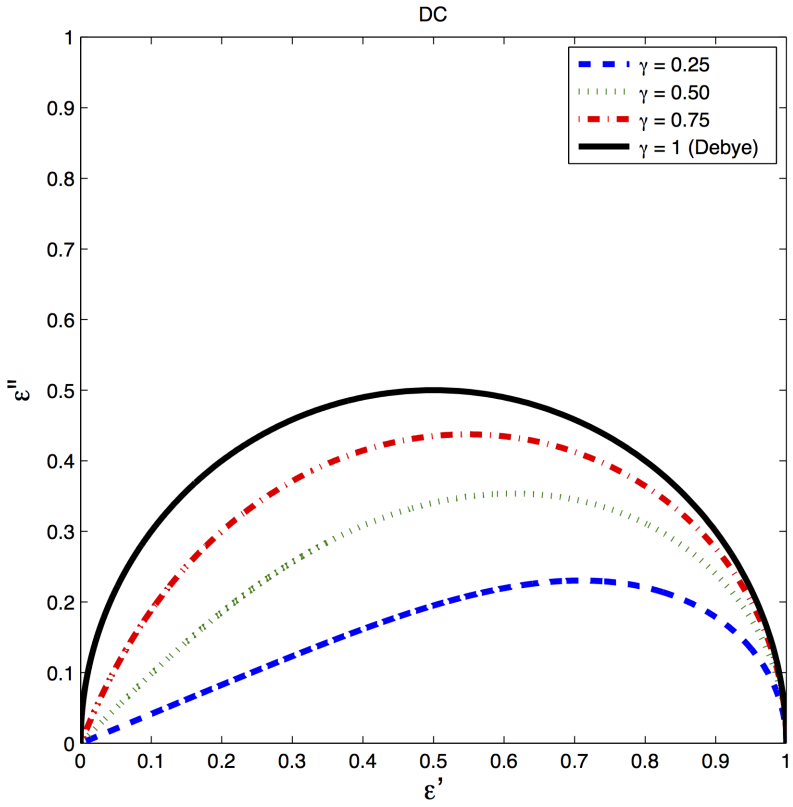

Figure 4.3: Plot of normalized permettivity $\frac{(\varepsilon'_{DC}-\varepsilon_\infty)}{(\varepsilon_s-\varepsilon_\infty)}$ against loss factor $\frac{\varepsilon''_{DC}}{(\varepsilon_s-\varepsilon_\infty)}$ showing the charachteristic Davidson-Cole skewed arc for different values of γ, where the maximum in ε''_{DC} does not correspond with $\omega\tau = 1$; this point is found at the interception of the bisector of the high-frequency limiting angle with the data plot.

where the identity

$$\Gamma(\gamma)\Gamma(1-\gamma) = \frac{\pi}{\sin(\gamma\pi)} \tag{4.9}$$

was used.

The graphic in Figure 4.2 shows the behaviour of $K_{\text{D-C}}(r)$ for different values of the parameter γ.

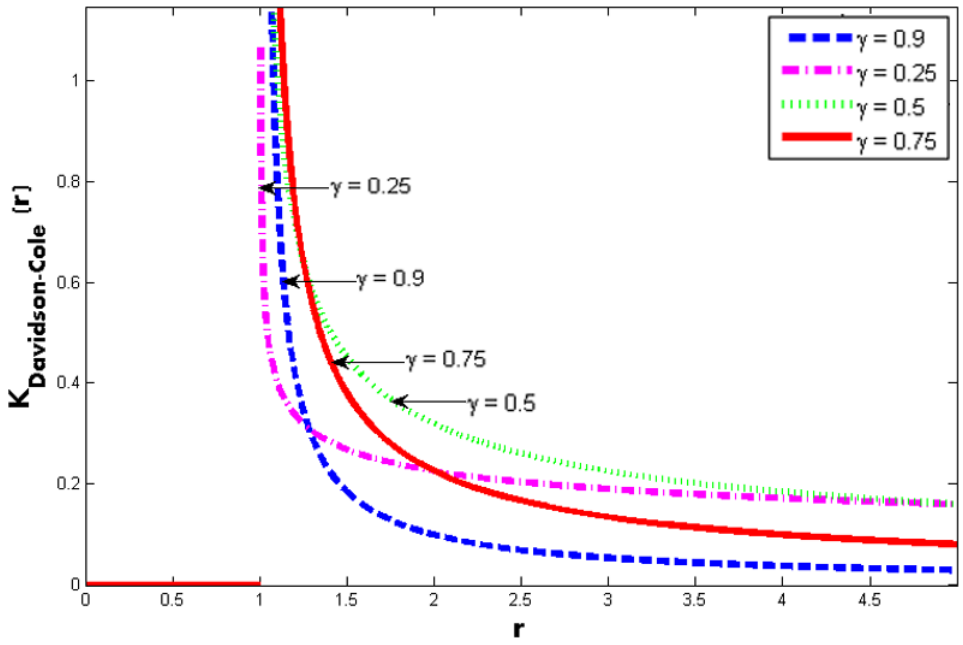

Figure 4.4: The spectral density for the Cole-Cole model $K_{\text{D-C}}(r) := K^{\gamma}_{1,\gamma}(r)$ calculated for $\gamma = 0.9$, $\gamma = 0.75$, $\gamma = 0.5$ and $\gamma = 0.25$.

4.3 Havriliak-Negami mathematical model

As seen in the previous sections, the Havriliak-Negami (H-N) relaxation model is a non-Debye relaxation model too, depending on two parameters, $\alpha \in]0,1[$ and $\gamma \in]0,1[$, that for $\alpha = \gamma = 1$ reduces to the standard Debye model. Taking into account (4.1) and (3.28), the response function can be written as:

$$\xi_{\text{H-N}}(t) = t^{\alpha\gamma-1}\, E^{\gamma}_{\alpha,\alpha\gamma}(-t^{\alpha}) \tag{4.10}$$

while, according to (3.29), its Laplace transform is:

$$\widetilde{\xi}_{\text{H-N}}(s) = \frac{1}{(1+s^{\alpha})^{\gamma}}\,. \tag{4.11}$$

Comparing (4.7) with (2.11), it is easy to find the same structure for the complex permettivity with the suitable change of variable. We note that this model for $\alpha \in]0,1[$ and $\gamma = 1$ reduces to the Cole-Cole model of (4.2) and (4.3), while for $\alpha = 1$ and $\gamma \in]0,1[$ to the Davidson-Cole model of (4.6) and

(4.7). We also recognize that whereas for the Cole-Cole and Havriliak-Negami models the corresponding response functions decay like a certain negative power of time (namely $t^{-\alpha-1}$ for a Tauberian theorem), the Davidson-Cole response function exhibits an exponential decay being $\alpha = 1$.

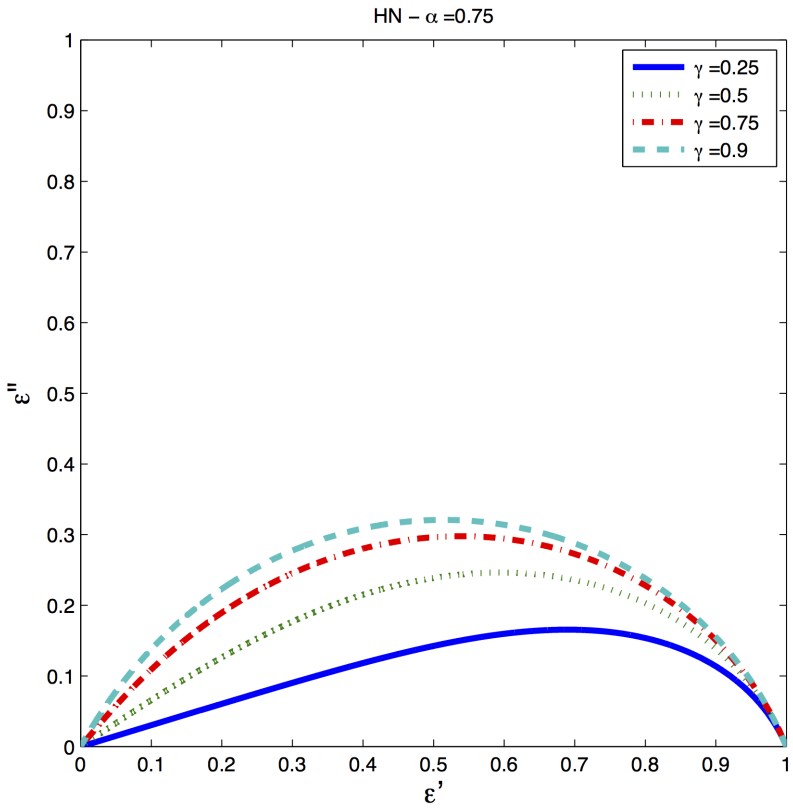

Figure 4.5: Plot of normalized permettivity $\frac{(\varepsilon'_{HN}-\varepsilon_\infty)}{(\varepsilon_s-\varepsilon_\infty)}$ against loss factor $\frac{\varepsilon''_{HN}}{(\varepsilon_s-\varepsilon_\infty)}$ showing that, as with the Davidson-Cole plot, the $\omega\tau = 1$ point is found at the interception of the bisector of the high-frequency limiting angle with the data plot.

The Cole-Cole plot of this model is displayed in Figure 4.5 where it is easy to note that it is an asymmetric curve intercepting real axis at different angles at high and low frequencies.

To derive the spectral density for the Havriliak-Negami model, the (3.31)

is used obtaining (3.33):

$$K_{\text{H-N}}(r) := K^{\gamma}_{\alpha,\alpha\gamma}(r) = \frac{1}{\pi}\frac{1}{(r^{2\alpha} + 2r^{\alpha}\,\cos(\alpha\pi) + 1)^{\frac{\gamma}{2}}}\sin\left[\gamma\arctan\left(\frac{r^{\alpha}\sin(\pi\alpha)}{r^{\alpha}\cos(\pi\alpha) + 1}\right)\right]. \tag{4.12}$$

In Figures 4.6 and 4.7 it is showed the behaviour of $K_{\text{H-N}}(r)$ for $\alpha = 0.5$ and $\alpha = 0.75$ and for different values of the parameter γ.

In equation (4.12) we can rename a factor in the argument of sine function; in particular:

$$\theta_{\alpha}(r) := \arctan\left(\frac{r^{\alpha}\sin(\pi\alpha)}{r^{\alpha}\cos(\pi\alpha) + 1}\right) = \arctan(\chi_{\alpha})\,. \tag{4.13}$$

The plot of this function, for three different values of α is drawn in graphic in Figure 4.8.

For big values of r, its asymptotic behaviour is:

$$\theta_{\alpha}(r) = \pi\alpha\,, \tag{4.14}$$

because its argument reduces to:

$$\chi_{\alpha}(r) = \frac{r^{\alpha}\sin(\pi\alpha)}{r^{\alpha}\cos(\pi\alpha) + 1} = \frac{\sin(\pi\alpha)}{\cos(\pi\alpha) + \frac{1}{r^{\alpha}}} \xrightarrow{r\to\infty} \frac{\sin(\pi\alpha)}{\cos(\pi\alpha)} = \tan(\pi\alpha)\,. \tag{4.15}$$

It is interesting to examine also the sine function in (4.12):

$$\phi_{\alpha}(r) := \sin(\gamma\theta_{\alpha}(r)) = \sin(\gamma\arctan(\chi_{\alpha})) \tag{4.16}$$

whose curve trend is showed in Figure 4.9.

As explained before, in order to avoid discontinuities in arctangent, if its argument becomes negative, we have to add π.
When $\chi_{\alpha}(r) > 0$, we have $\theta_{\alpha}(r) \leq \pi/2$ and, of course, $\phi_{\alpha}(r) = \sin(\gamma\theta_{\alpha}(r)) \leq i$ since $\gamma \in]0, 1[$. This the reason behind the fact that the graphic in Figure 4.9 doesn't show the charachteristic oscillations typical of sine function, never reaching its maximum value.
When $\chi < 0$, we have to add a π as seen in (3.35) and the added π is balanced by the negative values of arctangent function. In fact:

$$-\frac{\pi}{2} < \arctan\chi_{\alpha} < 0 \qquad \Longrightarrow \qquad \frac{\pi}{2} < \arctan\chi_{\alpha} + \pi < \pi\,. \tag{4.17}$$

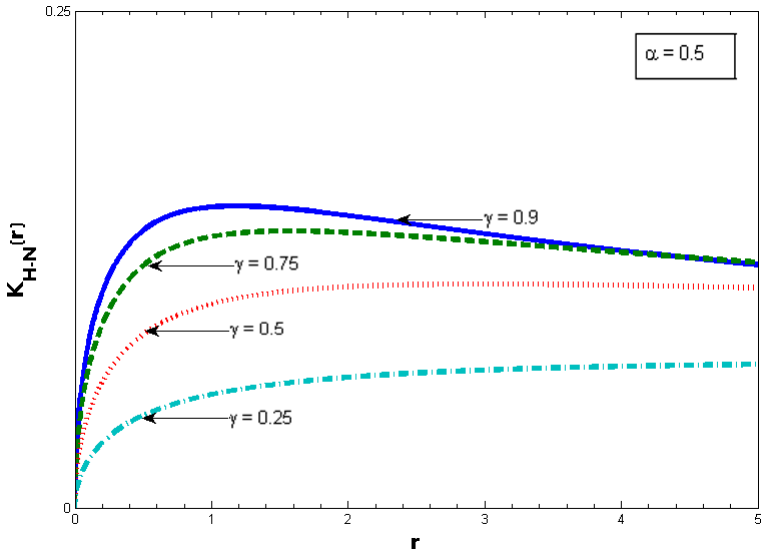

Figure 4.6: The spectral density for the Havriliak-Negami model $K_{\text{H-N}}(r) := K^{\gamma}_{1/2,\gamma/2}(r)$ calculated for $\gamma = 0.9$, $\gamma = 0.75$, $\gamma = 0.5$ and $\gamma = 0.25$.

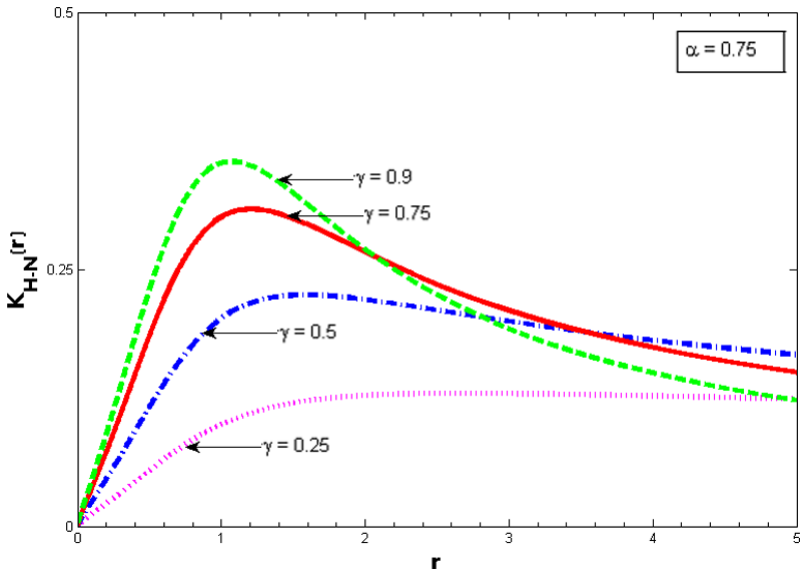

Figure 4.7: The spectral density for the Havriliak-Negami model $K_{\text{H-N}}(r) := K^{\gamma}_{3/4,3\gamma/4}(r)$ calculated for $\gamma = 0.9$, $\gamma = 0.75$, $\gamma = 0.5$ and $\gamma = 0.25$.

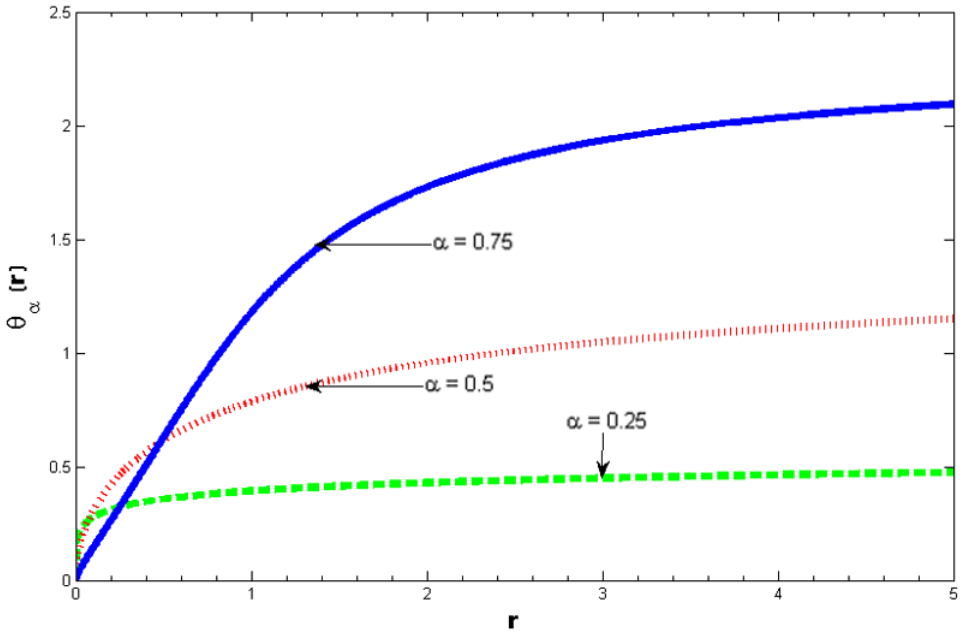

Figure 4.8: The function $\theta_\alpha(r)$ calculated for $\alpha = 0.75$, $\alpha = 0.5$ and $\alpha = 0.25$.

So $\sin(\gamma\theta_\alpha(r)) = \sin(\gamma \arctan\chi + \gamma\pi)$ begins exactly in the last point where the arctangent argument was positive, and after having reached its maximum value it starts to decrease, as we can easily note in Figure 4.6, or even better in Figure 4.7.

For completness, we show also the arctangent argument $\chi_\alpha(r) = \frac{r^\alpha \sin(\pi\alpha)}{r^\alpha \cos(\pi\alpha)+1}$, plotted in Figure 4.10, noting that $\chi_\alpha(r) < 0$ (so we have to add π to $\theta_\alpha(r)$) when the denominator $r^\alpha \cos(\pi\alpha) + 1$ becomes negative.

As well as we did for the Cole-Cole relaxation model, we can evaluate the maximum of the spectral density also for Havriliak-Negami, found where:

$$\gamma \arctan\left(\frac{r^\alpha \sin(\pi\alpha)}{r^\alpha \cos(\pi\alpha) + 1}\right) = \arctan\left(\frac{\sin(\pi\alpha)}{\cos(\pi\alpha) + r^\alpha}\right), \tag{4.18}$$

that for $\gamma = 1$ reduces to the trivial case $r = 1$ of Cole-Cole model, while for different cases it requires a numerical treatment, because of its two parameters dependence.

In conclusion, we evaluate that the complete monotonicity is ensured when $\alpha\gamma < 1$, so γ can overcome the value 1 and not only be restricted in

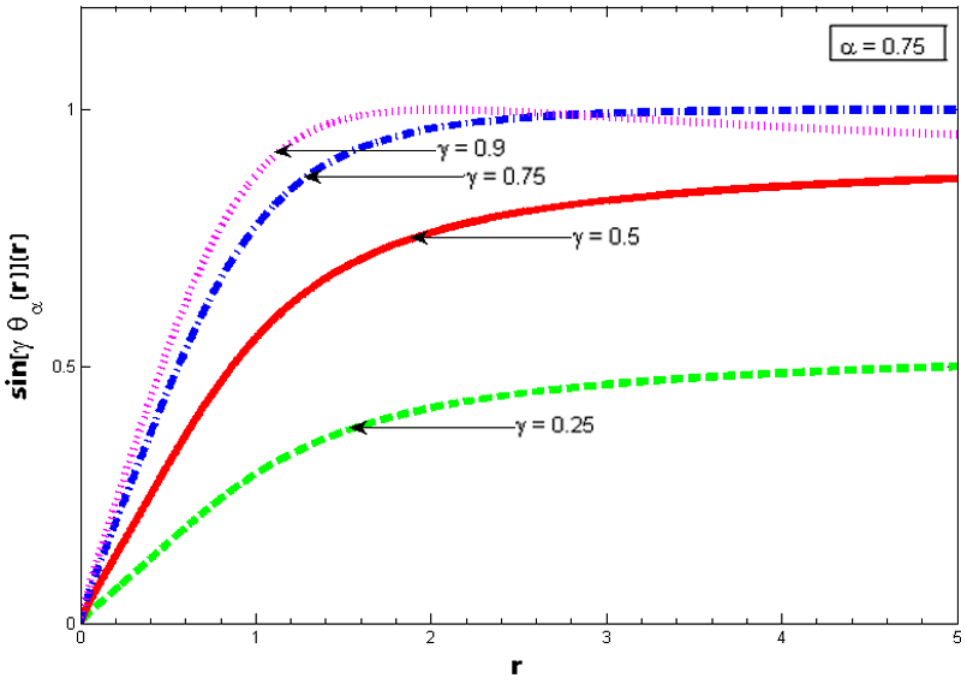

Figure 4.9: $\phi_\alpha(r)$ calculated for a fixed $\alpha = 0.75$ and for $\gamma = 0.9$, $\gamma = 0.75$, $\gamma = 0.5$ and $\gamma = 0.25$.

]0,1[. In Figures 4.11 and 4.12 there are the plots of $K_{\text{H-N}}(r)$ for $1 \leq \gamma < 1/\alpha$, while in Figures 4.13, 4.14 and 4.15 are shown the Cole-Cole plots for $\alpha = 0.25$, $\alpha = 0.5$ and $\alpha = 0.75$ for some values of γ exceeding 1, differently from what was done in Chapter 2 and represented in the Cole-Cole plots in Figure 4.5.

4.4 General case

After having studied the three classical models of Cole-Cole, Davidson-Cole and Havriliak-Negami according to the scheme in (4.1), we are now interested in more general cases, when the inequalities (3.32) become true in the most general sense, without the restrictions provided by the models mentioned above.

So, we must not restrict our attention to values of $\gamma \in]0, 1]$, because

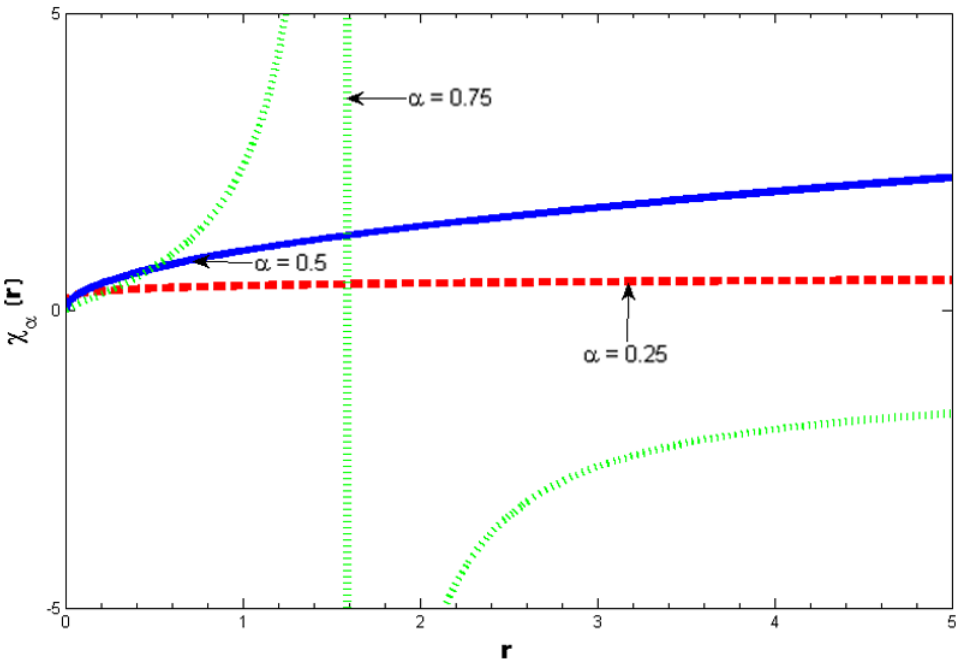

Figure 4.10: $\chi_\alpha(r)$ calculated for $\alpha = 0.75$, $\alpha = 0.5$ and $\alpha = 0.25$.

we are interesting in watching the behaviour of the spectral density $K^\gamma_{\alpha,\beta}(r)$ when $\gamma > 1$ and when $0 < \alpha < 1$ and $0 < \alpha\gamma \leq \beta \leq 1$ are valid.

The first thing that is possible to note in Figures 4.16,4.17, 4.18, and 4.19 is the divergence near the origin; this is explicable looking at the inequality $\alpha\gamma \leq \beta$ that makes $r^{|\alpha\gamma-\beta|}$ the driving term in (3.31) near the origin.

Then, for little r, the sine can cause a pair of oscillations while, increasing r, the polinomial denominator takes over.

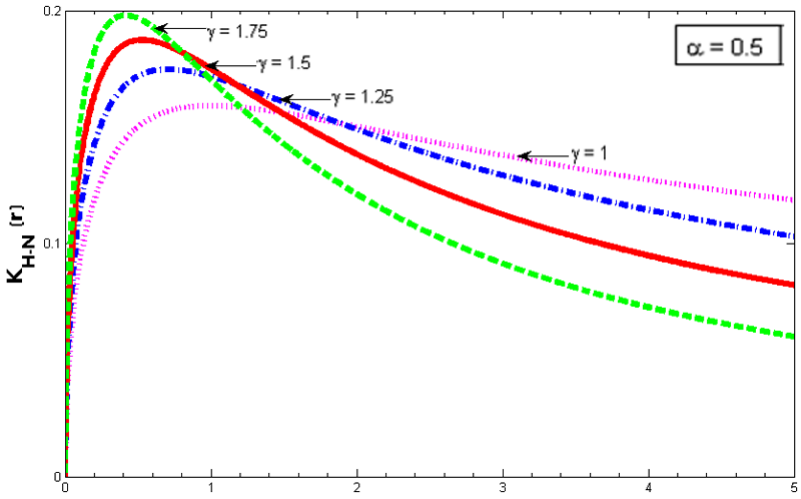

Figure 4.11: The spectral density for the Havriliak-Negami model $K_{\text{H-N}}$ for a fixed $\alpha = 0.5$ calculated for four values of $\gamma < 2$: $\gamma = 1.75$, $\gamma = 1.5$, $\gamma = 1.25$ and $\gamma = 1$.

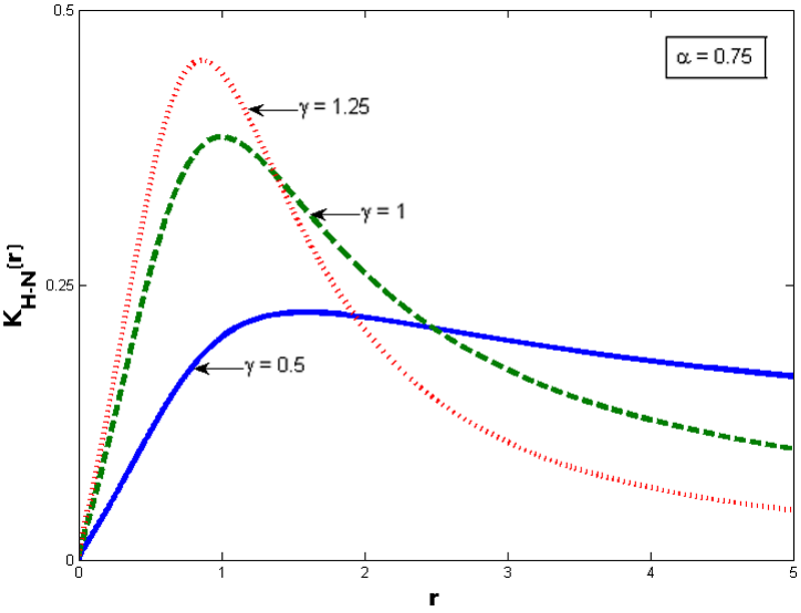

Figure 4.12: The spectral density for the Havriliak-Negami model $K_{\text{H-N}}$ for a fixed $\alpha = 0.75$ calculated for three values of $\gamma < 4/3$: $\gamma = 1.25$, $\gamma = 1$, $\gamma = 0.5$ and $\gamma = 1$.

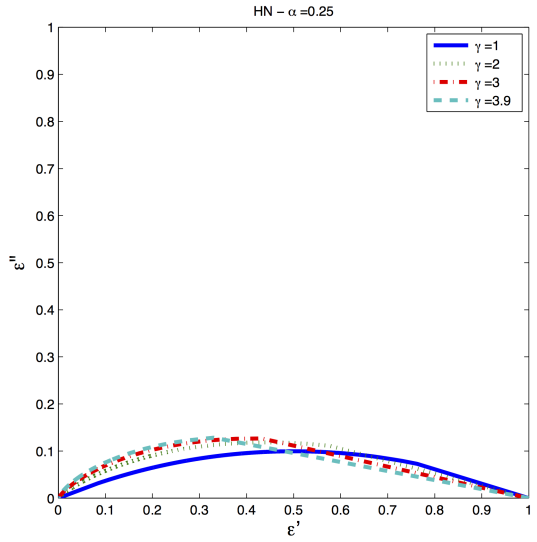

Figure 4.13: Cole-Cole plot for Havriliak-Negami model for $\alpha = 0.25$ and $\gamma < 4$, satisfying the condition $\alpha\gamma < 1$.

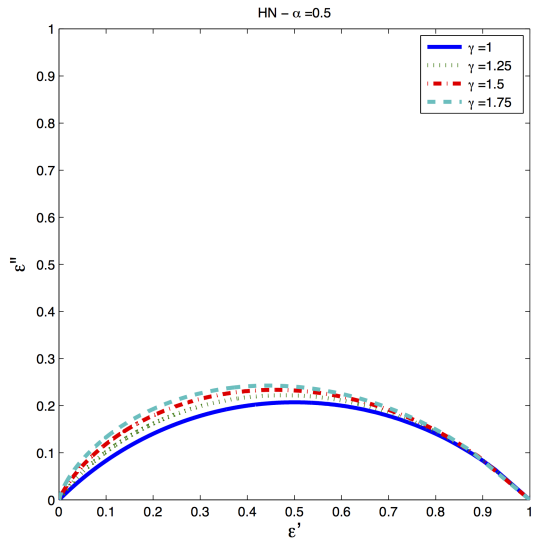

Figure 4.14: Cole-Cole plot for Havriliak-Negami model for $\alpha = 0.5$ and $\gamma < 2$, satisfying the condition $\alpha\gamma < 1$.

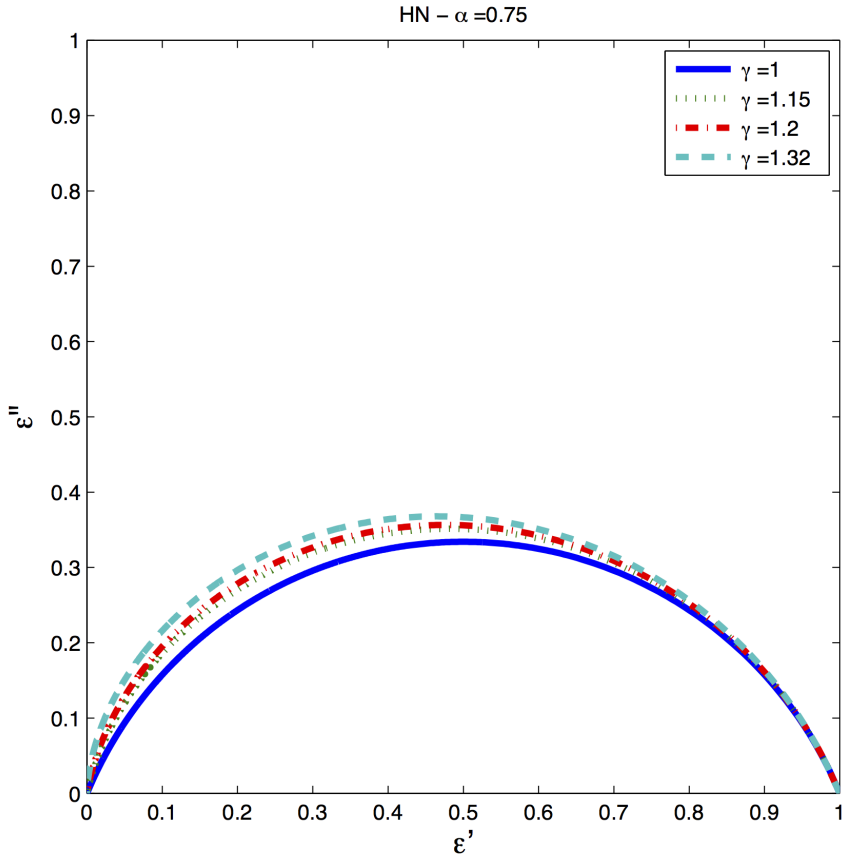

Figure 4.15: Cole-Cole plot for Havriliak-Negami model for $\alpha = 0.75$ and $\gamma < 1.333$, satisfying the condition $\alpha\gamma < 1$.

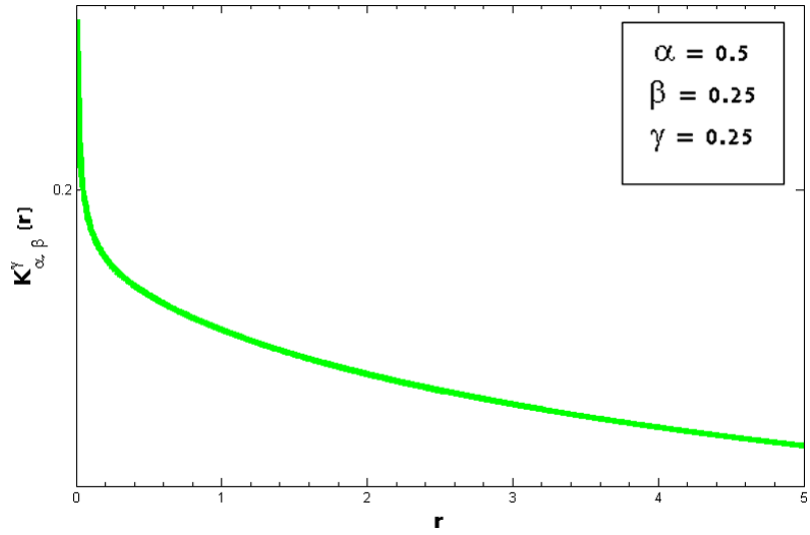

Figure 4.16: The spectral density $K^{\gamma}_{\alpha,\beta}(r)$ calculated for $\alpha = 0.5$, $\beta = 0.25$ and $\gamma = 0.25$.

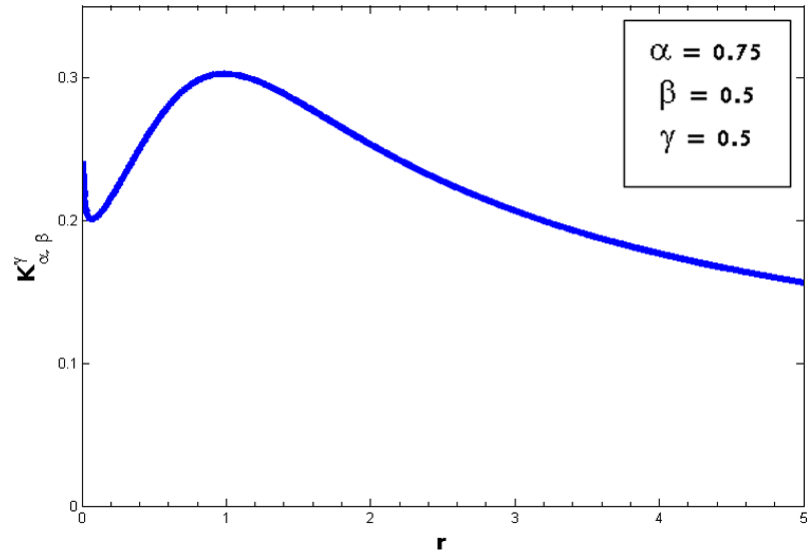

Figure 4.17: The spectral density $K^{\gamma}_{\alpha,\beta}(r)$ calculated for $\alpha = 0.75$, $\beta = 0.5$ and $\gamma = 0.5$.

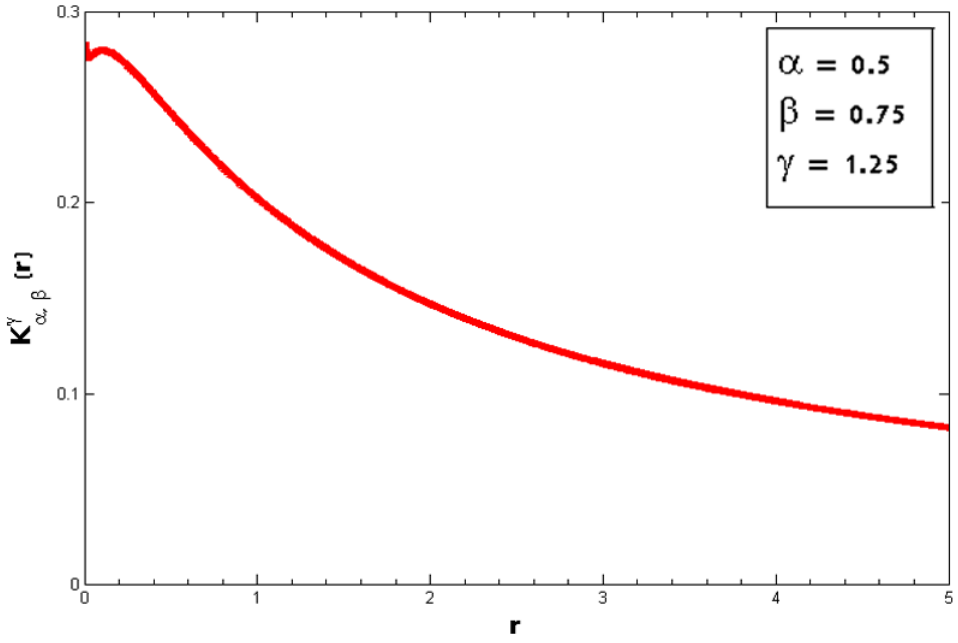

Figure 4.18: The spectral density $K^{\gamma}_{\alpha,\beta}(r)$ calculated for $\alpha = 0.5$, $\beta = 0.75$ and $\gamma = 1.25$.

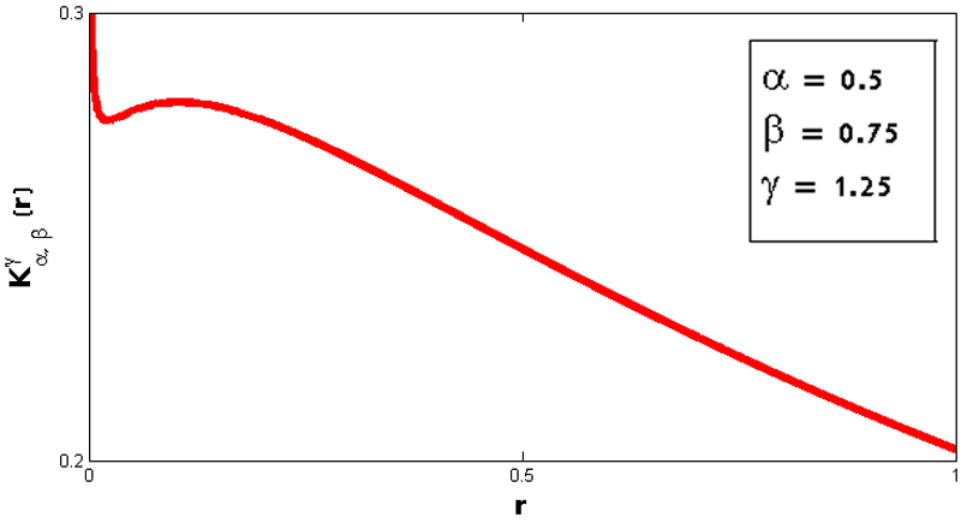

Figure 4.19: The behaviour near the origin of the spectral density $K^{\gamma}_{\alpha,\beta}(r)$ calculated for $\alpha = 0.5$, $\beta = 0.75$ and $\gamma = 1.25$.

Appendix A

Three parameters spectral density

In this appendix we collect some details regarding the derivation of the spectral density $K^{\gamma}_{\alpha,\beta}(r)$. Considering the Titchmarsh inversion formula (3.21) and applying it to the Laplace transform of the Mittag-Leffler we have:

$$\begin{aligned} K^{\gamma}_{\alpha,\beta}(r) &= \frac{r^{-\beta}}{\pi}\,\mathrm{Im}\left\{\mathrm{e}^{i\beta\pi}\left(\frac{r^{\alpha}+\mathrm{e}^{-i\alpha\pi}}{r^{\alpha}+2\cos(\alpha\pi)+r^{-\alpha}}\right)^{\gamma}\right\} \\ &= -\frac{r^{\alpha\gamma-\beta}}{\pi}\,\mathrm{Im}\left\{\frac{\mathrm{e}^{i(\alpha\gamma-\beta)\pi}}{(r^{\alpha}\mathrm{e}^{i\alpha\pi}+1)^{\gamma}}\right\} \\ &= -\frac{r^{\alpha\gamma-\beta}}{\pi}\,\mathrm{Im}\left\{\frac{\mathrm{e}^{i(\alpha\gamma-\beta)\pi}}{(r^{\alpha}\mathrm{e}^{i\alpha\pi}+1)^{\gamma}}\frac{(r^{\alpha}\mathrm{e}^{-i\alpha\pi}+1)^{\gamma}}{(r^{\alpha}\mathrm{e}^{-i\alpha\pi}+1)^{\gamma}}\right\} \end{aligned}$$

It is not difficult to check that in the above expression the denominator is real because:

$$\begin{aligned} (r^{\alpha}\mathrm{e}^{i\alpha\pi}+1)^{\gamma}(r^{\alpha}\mathrm{e}^{i\alpha\pi}+1)^{\gamma} &= (r^{2\alpha}+r^{\alpha}\mathrm{e}^{i\alpha\pi}+r^{\alpha}\mathrm{e}^{-i\alpha\pi}+1)^{\gamma} \\ &= (r^{2\alpha}+r^{\alpha}(\mathrm{e}^{i\alpha\pi}+\mathrm{e}^{-i\alpha\pi})+1)^{\gamma} \\ &= (r^{2\alpha}+2r^{\alpha}\cos(\alpha\pi)+1)^{\gamma} \qquad \in \mathbb{R}\,, \end{aligned}$$

so we can define:

$$(r^{\alpha}\mathrm{e}^{i\alpha\pi}+1)(r^{\alpha}\mathrm{e}^{-i\alpha\pi}+1) = r^{2\alpha}+2r^{\alpha}\,\cos(\alpha\pi)+1 =: \xi\,,$$

with

$$\xi \geq (r^{\alpha}-1)^2 \geq 0\,,$$

so that

$$\xi^{\frac{\gamma}{2}} \in \mathbb{R}\,.$$

Looking at the numerator we can compute:

$$(r^{\alpha}\mathrm{e}^{-i\alpha\pi}+1) =: z = \rho\mathrm{e}^{-i\theta}\,,$$

where

$$\rho = |z| = \sqrt{\mathrm{Re}^2 z + \mathrm{Im}^2 z} = \xi^{\frac{1}{2}}$$

and

$$\tan\theta = -\frac{\mathrm{Im}z}{\mathrm{Re}z} = \frac{r^{\alpha}\sin(\pi\alpha)}{r^{\alpha}\cos(\pi\alpha)+1}\,.$$

We can now use the The Moivre's formula:

$$(\cos\psi + i\sin\psi)^n = \cos(n\psi) + i\sin(n\psi)$$

and write:

$$\begin{aligned}
K^{\gamma}_{\alpha,\beta}(r) &= -\frac{r^{\alpha\gamma-\beta}}{\pi}\,\mathrm{Im}\left\{\frac{\mathrm{e}^{i(\alpha\gamma-\beta)\pi}}{(r^{\alpha}\mathrm{e}^{i\alpha\pi}+1)^{\gamma}}\frac{(r^{\alpha}\mathrm{e}^{-i\alpha\pi}+1)^{\gamma}}{(r^{\alpha}\mathrm{e}^{-i\alpha\pi}+1)^{\gamma}}\right\}\\
&= -\frac{r^{\alpha\gamma-\beta}}{\pi}\,\mathrm{Im}\left\{\frac{\mathrm{e}^{i(\alpha\gamma-\beta)\pi}(\rho\mathrm{e}^{-i\theta})^{\gamma}}{\xi^{\gamma}}\right\}\\
&= -\frac{r^{\alpha\gamma-\beta}}{\pi\xi^{\gamma}}\,\mathrm{Im}\{\Big[\cos[(\alpha\gamma-\beta)\pi]+i\sin[(\alpha\gamma-\beta)\pi]\Big]\rho^{\gamma}\Big(\cos\theta - i\sin\theta\Big)^{\gamma}\}\\
&= -\frac{r^{\alpha\gamma-\beta}}{\pi\xi^{\gamma}}\,\mathrm{Im}\{\Big[\cos[(\alpha\gamma-\beta)\pi]+i\sin[(\alpha\gamma-\beta)\pi]\Big]\xi^{\gamma/2}\Big(\cos(\gamma\theta) - i\sin(\gamma\theta)\Big)\}\\
&= -\frac{r^{\alpha\gamma-\beta}}{\pi\xi^{\gamma/2}}\,\mathrm{Im}\{\cos[(\alpha\gamma-\beta)\pi]\cos(\gamma\theta) + i\sin[(\alpha\gamma-\beta)\pi]\cos(\gamma\theta)+\\
&\qquad\qquad - i\cos[(\alpha\gamma-\beta)\pi]\sin(\gamma\theta) + \sin[(\alpha\gamma-\beta)\pi]\sin(\gamma\theta)\}\\
&= -\frac{r^{\alpha\gamma-\beta}}{\pi\xi^{\gamma/2}}\,\Big[\sin[(\alpha\gamma-\beta)\pi]\cos(\gamma\theta) - \cos[(\alpha\gamma-\beta)\pi]\sin(\gamma\theta)\Big]\\
&= -\frac{r^{\alpha\gamma-\beta}}{\pi\xi^{\gamma/2}}\,\sin[(\alpha\gamma-\beta)\pi - \gamma\theta]\\
&= \frac{r^{\alpha\gamma-\beta}}{\pi\xi^{\gamma/2}}\,\sin[(\beta-\alpha\gamma)\pi + \gamma\theta]\,,
\end{aligned}$$

where

$$\theta = \theta_\alpha(r) := \arctan\left[\frac{r^\alpha \sin(\pi\alpha)}{r^\alpha \cos(\pi\alpha) + 1}\right] \in [0, \pi]\,.$$

Substituting the expressions of θ and ξ in the above result, we find exactly (3.31) that we write again here for clearness:

$$K^\gamma_{\alpha,\beta}(r) = \frac{1}{\pi} \frac{r^{\alpha\gamma-\beta}}{(r^{2\alpha} + 2r^\alpha\, \cos(\alpha\pi) + 1)^{\frac{\gamma}{2}}} \sin\left[\gamma \arctan\left(\frac{r^\alpha \sin(\pi\alpha)}{r^\alpha \cos(\pi\alpha) + 1}\right) + (\beta - \alpha\gamma)\pi\right]$$

quod erat demonstrandum.

Appendix B

Formal demonstration of $K^1_{\alpha,\beta}(r) = K_{\alpha,\beta}(r)$

In this appendix we show how, for $\gamma = 1$, the spectral density of 3-parameters Mittag-Leffler function $K^{\gamma}_{\alpha,\beta}(r)$ reduces to the 2-parameters spectral density $K_{\alpha,\beta}(r)$. Recalling (3.31), for $\gamma = 1$ we have:

$$\begin{aligned} K^1_{\alpha,\beta}(r) &= \frac{1}{\pi} \frac{r^{\alpha-\beta}}{(r^{2\alpha} + 2r^{\alpha}\,\cos(\alpha\pi) + 1)^{\frac{\gamma}{2}}} \sin\left[\arctan\left(\frac{r^{\alpha}\sin(\pi\alpha)}{r^{\alpha}\cos(\pi\alpha)+1}\right) + (\beta-\alpha)\pi\right] \\ &= \frac{1}{\pi} \frac{r^{\alpha-\beta}}{\xi^{1/2}} \sin[\theta + (\beta-\alpha)\pi]\,, \end{aligned}$$

where we call $\xi = r^{2\alpha} + 2r^{\alpha}\,\cos(\alpha\pi) + 1$, and $\theta = \arctan\left(\frac{r^{\alpha}\sin(\pi\alpha)}{r^{\alpha}\cos(\pi\alpha)+1}\right)$ as well as in Appendix A, just for brevity.

Recalling the trigonometric formula $\sin(\alpha+\beta) = \sin(\alpha)\cos(\beta)+\cos(\alpha)\sin(\beta)$, we have:

$$\begin{aligned} K^1_{\alpha,\beta}(r) &= \frac{1}{\pi} \frac{r^{\alpha-\beta}}{\xi^{\frac{1}{2}}} \Big[\sin\theta\cos(\beta-\alpha)\pi + \cos\theta\sin(\beta-\alpha)\pi\Big] \\ &= \frac{1}{\pi} \frac{r^{\alpha-\beta}}{\xi^{\frac{1}{2}}} \cos\theta \Big[\tan\theta\cos(\beta-\alpha)\pi + \sin(\beta-\alpha)\pi\Big] \\ &= \frac{1}{\pi} \frac{r^{\alpha-\beta}}{\xi^{\frac{1}{2}}} \cos\theta \left[\frac{r^{\alpha}\sin(\pi\alpha)}{r^{\alpha}\cos(\pi\alpha)+1}\cos(\beta-\alpha)\pi + \sin(\beta-\alpha)\pi\right]. \end{aligned}$$

Noting that

$$\tan^2\theta = \left(\frac{r^\alpha \sin(\pi\alpha)}{r^\alpha \cos(\pi\alpha)+1}\right)^2 = \frac{\sin^2\theta}{\cos^2\theta} = \frac{1-\cos^2\theta}{\cos^2\theta} = \frac{1}{\cos^2\theta} - 1$$

we can write:

$$\cos^2\theta = \frac{1}{\tan^2\theta+1} = \frac{\left(r^\alpha\cos(\pi\alpha)+1\right)^2}{r^{2\alpha}\left(\sin^2(\pi\alpha)+\cos^2(\pi\alpha)\right)+2r^\alpha\cos(\pi\alpha)+1} = \frac{\left(r^\alpha\cos(\pi\alpha)+1\right)^2}{\xi}\,.$$

Extracting the square root we find:

$$\begin{aligned}
K^1_{\alpha,\beta}(r) &= \frac{1}{\pi}\frac{r^{\alpha-\beta}}{\xi^{\frac{1}{2}}}\left(\frac{r^\alpha\cos(\pi\alpha)+1}{\xi^{\frac{1}{2}}}\right)\left[\frac{r^\alpha\sin(\pi\alpha)}{r^\alpha\cos(\pi\alpha)+1}\cos(\beta-\alpha)\pi+\sin(\beta-\alpha)\pi\right] \\
&= \frac{1}{\pi}\frac{r^{\alpha-\beta}}{\xi}\Big[r^\alpha\sin(\pi\alpha)\cos(\beta-\alpha)\pi + r^\alpha\cos(\pi\alpha)\sin(\beta-\alpha)\pi+\sin(\beta-\alpha)\pi\Big] \\
&= \frac{1}{\pi}\frac{r^{\alpha-\beta}}{\xi}\Big[r^\alpha\sin(\beta\pi)+\sin(\beta-\alpha)\pi\Big] \\
&= \frac{r^{\alpha-\beta}}{\pi}\,\frac{\sin\left[(\beta-\alpha)\pi\right]+r^\alpha\,\sin\left(\beta\pi\right)}{r^{2\alpha}+2r^\alpha\,\cos(\alpha\pi)+1} = K_{\alpha,\beta}(r)
\end{aligned}$$

quod erat demonstrandum.

Appendix C

Completely monotonic and Bernstein functions

In this appendix we list a number of definitions and basic properties related to two special classes of functions that have been treated in Chapter 2 because of their importance in our discussion of the mathematical models behind the phenomen of dielectric relaxation. The two types of function we are going to investigate are the Completely Monotonic (CM) and the Bernstein (B) functions with their sub-classes: the Stieltjes (SCM) and the Completely Bernstein (CB) functions, respectively.

All these functions are real-valued and defined in $\mathbb{R}^+$ where they possess infinitely many derivatives that are of class C^∞. When subjected to Laplace transformation, the functions are required to be sufficiently well behaved and Locally Integrable (LI).

C.1 Basic definitions and properties

We recall that a real-valued function $\phi(t)$ defined for $t \geq 0$ is said to be completely monotonic (CM) if it is a non-negative function with infinitely many derivatives alternated in sign:

$$\phi(t) \geq 0\,, \quad (-1)^n \frac{d^n}{dt^n}\,\phi(t) \geq 0\,, \quad n = 0, 1, 2, ..., \quad t \geq 0\,. \tag{C.1}$$

A function $\psi(t)$ defined for $t \geq 0$ is said to be Bernstein (B) if it is non-negative and its first derivative is CM:

$$\psi(t) \geq 0\,, (-1)^{n-1}\frac{d^n}{dt^n}\,\psi(t) \geq 0\,,\ n = 1, 2, ...,\quad t \geq 0\,. \tag{C.2}$$

The limits of $\phi(t)$ and $\psi(t)$ and their derivatives are assumed exist, finite or infinite. Henceforth, for $t > 0$ a CM function is non-negative, non-increasing and convex, whereas a B function is non-negative, non-decreasing and concave. Their prototypes and simplest examples are respectively:

$$\phi(t) = \exp(-t)\,,\quad \psi(t) = 1 - \exp(-t)\,,\quad t > 0\,. \tag{C.3}$$

From the definition it follows that, if $\phi(t)$ is CM and $\phi^{(n_0)}(t_0) = 0$ at some point $t_0 \in (0, \infty)$ for some $n_0 = 0, 1, 2, \ldots$, then its derivatives of greater order are also equal to zero at this point. A trivial observation is the $\phi(t)$ is CM, then $\phi^{(2m)}(t)$ and $-\phi^{(2m+1)}(t)$ are also CM for $m = 0, 1, 2, \ldots$.

The basic properties of CM and B functions that we first point out are related to the Bernstein theorem which provides their representation in terms of Laplace-Stieltjes transforms in the Lebesgue integration sense or in terms of Laplace transforms of locally integrable functions or of generalized functions.

- A function $\phi(t)$ is CM if and only if it can be represented as the Laplace-Stieltjes transform as follows

$$\phi(t) \text{ CM function} \iff \phi(t) = \int_0^\infty \mathrm{e}^{-rt}\,\mathrm{d}P(r)\,, \tag{C.4}$$

  where the integral converges for $0 < t < \infty$ and $P(r)$ is a non-decreasing function. This is the Widder's form of the Bernstein theorem mentioned above but the form we prefer to write, according to what we have done in Chapter 2, is different and is the following:

$$\phi(t) \text{ CM function} \iff \phi(t) = \int_0^\infty \mathrm{e}^{-rt}p(r)\,\mathrm{d}r\,,\ p(r) \geq 0\,, \tag{C.5}$$

  where $p(r)$ is an ordinary or generalized function. So, comparing (C.5) with (C.4), we can see that $p(r)$ is obtained differentiating (in ordinary

or generalized sense) the above function $P(r)$. More rigorously, $p(r)$ can be interpreted as the non-negative density of a suitable Borel or Radon measure on $[0, \infty[$.

Recalling the examples in (C.3), in the case $\phi(t) = \exp(-t)$ we have $p(r) = \delta(r-1)$, where δ denotes the Dirac generalized function.

We note that the $\Longleftarrow$ part of the Bernstein theorem is evident by differentiating under the integral. We also note that if $\lim_{t\to 0^+} \phi(t) = \infty$ then in (C.5) the spectral density $p(r)$ cannot be normalized being its integral $\int_0^\infty p(r)\, dr$ divergent.

- If a sequence of CM functions $f_n \longrightarrow f$ pointwise, then the limit f is a CM function. The proof of this fact is based on the Bernstein theorem.

- For a B function we have:

$$\psi(t) \text{ B function} \iff \psi(t) = a + b\,t + \int_0^\infty \left(1 - \mathrm{e}^{-rt}\right)\, q(r)\,\mathrm{d}r\,, \quad \text{(C.6)}$$

where

$$a = \psi(0^+)\,, \quad b = \lim_{t\to\infty} \frac{\psi(t)}{t}\,, \quad q(r) \geq 0\,. \qquad \text{(C.7)}$$

Here $q(r)$ is the non-negative density of a suitable Borel or Radon measure on $[0, \infty[$.

Recalling the examples in (C.3), in the case $\psi(t) = 1 - \exp(-t)$ we have $a = b = 0$ and $q(r) = \delta(r-1)$.

We note that if $\lim_{t\to+\infty} \psi(t) = \infty$ with $\psi(t) = o(t)$, then $b = 0$ and the spectral density $q(r)$ cannot be normalized being its integral $\int_0^\infty q(r)\, dr$ divergent.

If t denotes time, $p(r)$ and $q(r)$ are referred to as the frequency spectral densities of $\phi(t)$ and $\psi(t)$, because the dimensions of r are those of a frequency. They can be converted into spectral densities in time by replacing $r = \frac{1}{\tau}$ in the Laplace integrals carried out in τ. Then, distinguishing the spectral densities in frequency and in time by the

notation $\{p_r(r), q_r(r)\}$ and $\{p_\tau(\tau), q_\tau(\tau)\}$, we get respectively:

$$p_\tau(\tau) = \frac{p_r(\frac{1}{\tau})}{\tau^2}\,, \qquad q_\tau(\tau) = \frac{q_r(\frac{1}{\tau})}{\tau^2}\,. \tag{C.8}$$

Of course, by definition, $p_\tau(\tau)$ and $q_\tau(\tau)$ are non-negative (ordinary or generalized) functions like $p_r(r)$ and $q_r(r)$.

- There is a sort of inverse of the Bernstein theorem, according to which the inverse Laplace transform of a CM function is non-negative and viceversa, under suitable regularity conditions:

$$\phi(t) \geq 0\,, t \geq 0 \iff \widetilde{\phi}(s)\,\text{CM function}\,, s > 0\,, \tag{C.9}$$

where $\widetilde{\phi}(s)$ is the Laplace transform of $\phi(t)$ and, by definition,

$$\widetilde{\phi}(s) := \int_0^\infty \mathrm{e}^{-st}\,\phi(t)\,\mathrm{d}t\,. \tag{C.10}$$

This property is justified by the Post-Widder formula for the inversion of the Laplace transform:

$$\phi(t) = \lim_{n\to\infty} \frac{(-1)^n}{n!}\left(\frac{n}{t}\right)^{n+1} \widetilde{\phi}^{(n)}\left(\frac{n}{t}\right)\,. \tag{C.11}$$

- Linear combinations with non-negative weights and integrals with non-negative weights of CM and B functions are CM and B functions respectively. The same for the point-wise limit of convergent sequences and for products of CM and B functions. Moreover, also the product of the two CM functions in CM (this could be verified using the Leibniz formula).

- Let $\phi(t)$ be a CM function and let $\psi(t)$ a B function; the composite function $\phi[\psi(t)]$ is a CM function. This result is known as the Composition Theorem. In particular, the function $\mathrm{e}^{-\psi(t)}$ is CM if $\psi(t)$ is a Bernstein function.

- Further properties of CM functions come from the above Composition Theorem. For example we have the following two corrollaries:

$$f(t), g(t)\,\text{CM},\, a, b \geq 0 \implies f\left(a + b\int_0^t g(t')\,\mathrm{d}t'\right)\,\text{CM} \tag{C.12}$$

$$f(t)\ \text{CM},\ f(0) \leq A < \infty \implies \begin{cases} \frac{1}{[A-f(t)]^{\mu}}\ \text{CM} & \text{if} \quad \mu \geq 0, \\ -\log\left[1 - \frac{f(t)}{A}\right]\ \text{CM} \end{cases} \tag{C.13}$$

- If $\psi(t)$ is a B function, then $\psi(t)/t$ is CM.
- Let $y = \phi(t)$ be CM and let the power series

$$f(y) = \sum_{n=0}^{\infty} a_n\, y^n \tag{C.14}$$

converge for all y in the range of the function $y = \phi(t)$. If $a_n \geq 0$ for all $n = 0, 1, 2, \ldots$, then $f\,[\phi(t)]$ is CM.

C.2 The Gripenberg theorem

There is a theorem in particular that is of fundamental importance in treating the complete monotonicity of functions and its name is Gripenberg theorem.

It says that the Laplace transform $\widetilde{f}(s)$ of a unction $f(t)$ that is locally integrable on $\mathbb{R}^+$ and that is completely monotonic has the following properties:

1. $\widetilde{f}(s)$ has an analytical extension to the region $\mathbb{C} - \mathbb{R}^-$;
2. $\widetilde{f}(x) = \widetilde{f} * (x)$ for $x \in]0, \infty[$;
3. $\lim_{x\to\infty} \widetilde{f}(x) = 0$;
4. $\text{Im}\{\widetilde{f}(s)\} < 0$ for $\text{Im}\{s\} > 0$;
5. $\text{Im}\{s\widetilde{f}(s)\} \geq 0$ for $\text{Im}\{s\} > 0$ and $\widetilde{f}(x) \geq 0$ for $x \in]0, \infty[$.

Conversely, every function $\widetilde{f}(s)$ that satisfies (1)-(3) together with (4) or (5) is the Laplace transform of a function $f(t)$, which is locally integrable on $\mathbb{R}^+$ and completely monotonic on $]0, \infty[$.

The importance of the theorem is due to the fact that is provides necessary and sufficient conditions to ensure the completely monotonicity of a function $f(t)$ based on its Laplace transform $\widetilde{f}(s)$.

Now, as done by Capelas de Oliveira, Mainard and Vaz in [Capelas, Mainardi et al. 2014], we are using the inverse formulation of this theorem in order to provide a proof for the inequalities in (3.32) on the parameters α, β and γ required to ensure the non negativity of the spectral density $K^{\gamma}_{\alpha,\beta}(r)$:

$$0 < \alpha \leq 1\,, 0 < \beta \leq 1,\ 0 < \gamma \leq \frac{\beta}{\alpha} \Longleftrightarrow 0 < \alpha \leq 1\,, 0 < \alpha\gamma \leq \beta \leq 1,\,. \tag{C.15}$$

We recall the definitions of $\xi_G(t)$ and its Laplace transform $\widetilde{\xi}_G(s)$:

$$\xi_G(t) := t^{\beta-1} E^{\gamma}_{\alpha,\beta}(-t^{\alpha})\,, \tag{C.16}$$

and

$$\widetilde{\xi}_G(t) := \frac{s^{\alpha\gamma-\beta}}{(s^{\alpha}+1)^{\gamma}}\,. \tag{C.17}$$

We immediately recognize that the requirements (1)-(3) for $\widetilde{\xi}_G(s)$ are surely satisfied with the first two conditions in the left-hand side of (C.15), that is $0 < \alpha < 1$, $0 < \beta < 1$ but for any $\gamma > 0$. So for us it is enough to determine which additional condition is implied from the requirement (4) or (5) but we are using (4). We will prove that this relevant condition is just $0 < \alpha\gamma - \beta \leq 0$, namely $0 < \gamma \leq \frac{\beta}{\alpha}$, exactly as stated in (C.15).

Using (C.17), the requirement (4) reads:

$$\Lambda(s) := \mathrm{Im}\left[\frac{s^{\alpha\gamma-\beta}}{(s^{\alpha}+1)^{\gamma}}\right] < 0 \qquad \text{where} \qquad \mathrm{Im}\{s\} > 0\,. \tag{C.18}$$

Setting $s = r\mathrm{e}^{i\phi}$ in the complex upper half plane (since it has to be $\mathrm{Im}\{s\} > 0$) we consider:

$$\Lambda(r,\phi) := \mathrm{Im}\left[\frac{\left(r\mathrm{e}^{i\phi}\right)^{\alpha\gamma-\beta}\left(1+r^{\alpha}\mathrm{e}^{-i\alpha\phi}\right)^{\gamma}}{\left|1+r^{\alpha}\mathrm{e}^{-i\alpha\phi}\right|^{2\gamma}}\right] \quad \text{with} \quad r > 0 \,\text{and}\, 0 < \phi < \pi\,. \tag{C.19}$$

To prove that $\Lambda(r,\phi)$ is negative it is sufficient to consider the numerator because the denominator is always non-negative. Setting:

$$z := \left(r\mathrm{e}^{i\phi}\right)^{\alpha\gamma-\beta}\left(1+r^{\alpha}\mathrm{e}^{-i\alpha\phi}\right)^{\gamma} = \rho\mathrm{e}^{i\psi}\,, \tag{C.20}$$

we must verify that the conditions on α, β and γ stated in (C.15) ensure that z has a negative imaginary part, so ensure that it is located in the lower half plane with:

$$-\pi < \psi < 0\,. \tag{C.21}$$

Let:

$$z_1 = r^{\alpha\gamma-\beta}\mathrm{e}^{i(\alpha\gamma-\beta)\phi} = \rho_1\mathrm{e}^{i\psi_1}\,, \quad \rho_1 = r^{\alpha\gamma-\beta}\,, \quad \psi_1 = (\alpha\gamma-\beta)\phi\,, \tag{C.22}$$

$$z_2 = r^{\alpha}\mathrm{e}^{-i\alpha\phi} = \rho_2\mathrm{e}^{i\psi_2}\,, \quad \rho_2 = r^{\alpha}\,, \quad \psi_2 = -\alpha\phi \tag{C.23}$$

and

$$z_3 = (1+z_2)^{\gamma} = \rho_3\mathrm{e}^{i\psi_3}\,, \quad \rho_3 = \left|1 + r^{\alpha}\mathrm{e}^{-i\alpha\phi}\right|^{\gamma}\,, \quad -\alpha\gamma\phi < \psi_3 < 0\,. \tag{C.24}$$

So we can write the complex number in (C.20) as:

$$z = z_1 z_3 = \rho_1\mathrm{e}^{i\psi_1}\rho_3\mathrm{e}^{i\psi_3} = \rho\mathrm{e}^{i\psi}\,, \quad \rho = \rho_1\rho_3\,, \quad \psi = \psi_1 + \psi_3\,. \tag{C.25}$$

Now assuming $0 < \phi < \pi$, we find for $\alpha\gamma - \beta > 0$:

$$-(\beta - \alpha\gamma)\pi < \psi_1 < 0\,, \tag{C.26}$$

$$-\alpha\gamma\pi < \psi_3 < 0\,. \tag{C.27}$$

For $\alpha\gamma - \beta = 0$ we find $\psi_1 = 0$ and $-\alpha\gamma\pi = -\beta\pi < \psi_3 < 0$. As a consequence, for $\alpha\gamma - \beta \leq 0$ we finally get:

$$-\pi < -\beta\pi < \psi < 0\,, \tag{C.28}$$

so, since $0 < \beta < 1$, the inequality (C.21) is proved and as a consequence also the relation (C.15).

Appendix D

Entire functions

We dedicate this appendix to a schematical treatment of entire functions, linking them in particular to the subject of our mathematical analysis in the present work: the Mittag-Leffler function.

The period from 1850 to 1950 was, as written in [Gorenflo, Kilbas et al. 2014], the "golden century of the theory of entire functions"; theory that was one of the central subjects of complex analysis, developed in connection with se eral deep problems in mathematics as well as due to the usefulness of the analytic machinery for the solution of a wide range of applied problems. For example, Mittag-Leffler was interested in the solution of the analytic continuation problem as applied to the study of the convergence of divergent series. For this purpose he introduced a new entire function - the Mittag-Leffler function - which serves as the simplest generalization of the exponential function and also helped him to get a criterion for analytic continuation, generalizing results of many mathematicians before him.

But, before talking in particular about Mittag-Leffler function as an important example of entire function, we have to dedicate the following three sections about some important definitions.

D.1 Definition

A complex-valued function $F : \mathbb{C} \to \mathbb{C}$ is called *entire function* (or *integral function*) if it is analytic ($\mathbb{C}$-differentiable) everywhere on the complex plane; in other words the function is entire if at each point $z_0 \in \mathbb{C}$ the following limit exists:

$$\lim_{z \to z_0} \frac{F(z) - F(z_0)}{z - z_0} \in \mathbb{C}\,. \tag{D.1}$$

Typical examples of entire functions are the polynomials, the exponential functions and also sums product and composition of these functions, thus trigonometric and hyperbolic functions. Among special functions we have to point out the following entire functions: Airy functions $Ai(z), Bi(z)$, Bessel functions of first and second kind $J_\nu(z), Y_\nu(z)$, Fox H-functions $H_{p,q}^{m,n}(z)$ for certain values of parameters, reciprocal to gamma-function $\frac{1}{\Gamma(z)}$, generalized hypergeometric function ${}_pF_q(z)$, Meijer's G-functions $G_{p,q}^{m,n}(z)$, Mittag-Leffler function $E_\alpha(z)$ and its different generalizations, Wright function $\phi(z; \rho, \beta)$.

According to Liouville's theorem an entire function either has a singularity at infinity or it is a constant. Such singularity can be either a pole (the case of a polynomial), or an essential singularity. In this case we speak of *transcendental entire functions*. All above mentioned special functions are transcendental.

D.2 Series representations

Every entire function can be represented in the form of a power series

$$F(z) = \sum_{n=0}^{\infty} c_n z^n\,, \tag{D.2}$$

converging everywhere on $\mathbb{C}$.

According to the Cauchy-Hadamard formula, the coefficients of the series (D.2) satisfy the following condition that is also the necessary and sufficient condition for the sum of a power series to represent an entire function:

$$\lim_{n \to \infty} |c_n|^{\frac{1}{n}} = 0\,. \tag{D.3}$$

The absolute value of the coefficients of an entire function decreases necessarily to zero (although not monotonically, in general). One can classify the corresponding function in terms of the speed of this decrease. Thus

$$|c_n| \to 0 \quad \text{for} z \to \infty \tag{D.4}$$

is a necessary but not sufficient condition for convergence of a power series.

D.3 Order and type

The global behaviour of entire functions of finite order is characterized by their order and type. The *order* ρ of an entire function $F(z)$ is defined as an infimum of those n, for which the inequality

$$M_F(r) := \max_{|z|=r} |F(z)| < \mathrm{e}^{r^n}\,,\ \forall r > r(n) \tag{D.5}$$

holds. Equivalently:

$$\rho := \rho_F = \lim \sup_{r\to\infty} \frac{\ln \ln M_F(r)}{\ln r}\,. \tag{D.6}$$

Another characteristic of an entire function is its type. The *type* σ of an entire function $F(z)$ of finite order ρ is defined as an infinum of those $A > 0$ for which the inequality

$$M_F(r) < \mathrm{e}^{Ar^\rho},\ \forall r > r(n) \tag{D.7}$$

holds. Equivalently:

$$\sigma := \sigma_F = \lim \sup_{r\to\infty} \frac{\ln M_F(r)}{r^\rho}\,. \tag{D.8}$$

For an entire function $F(z)$ represented in the form (D.2), its order and type can be found using the following formulae:

$$\rho = \lim \sup_{n\to\infty} \frac{n \ln n}{\ln \frac{1}{|c_n|}}\,, \tag{D.9}$$

$$(\sigma \mathrm{e} \rho)^{\frac{1}{\rho}} = \lim\, sup_{n\to\infty} \left(n^{\frac{1}{\rho}} \sqrt[n]{|c_n|} \right)\,. \tag{D.10}$$

For instance, the exponential function e^z has the order $\rho = 1$ and the type $\sigma = 1$.

D.4 An example: the Mittag-Leffler function

Let us recall the 1-parameter Mittag-Leffler function already defined in (3.1) through a series representation:

$$E_\alpha(z) = \sum_{n=0}^{\infty} \frac{z^n}{\Gamma(\alpha n + 1)} \tag{D.11}$$

where $\alpha \in \mathbb{C}$. Comparing the formula above to (D.2), we can see that (D.2) can be recovered if the coefficients c_n are defined:

$$c_n := \frac{1}{\Gamma(\alpha n + 1)}\,. \tag{D.12}$$

Applying to these coefficients the Cauchy-Hadamard formula, the radius of convergence can be found as:

$$R = \limsup_{n\to\infty} \frac{|c_n|}{|c_{n+1}|}\,, \tag{D.13}$$

while the asymptotic formula is:

$$\frac{\Gamma(z+a)}{\Gamma(z+b)} = z^{a-b}\left[1 + \frac{(a-b)(a-b-1)}{2z} + O\left(\frac{1}{z^2}\right)\right] \quad (z\to\infty\,, |\arg z| < \pi)\,. \tag{D.14}$$

Taking into account these formulae, one can see that series in (D.11) converges in the whole complex plane for all $\mathrm{Re}\alpha > 0$, while for all $\mathrm{Re}\alpha < 0$ it diverges everywhere on $\mathbb{C}\setminus\{0\}$. For $\mathrm{Re}\alpha = 0$ the radius of convergence is equal to:

$$R = \mathrm{e}^{\frac{\pi}{2}|\mathrm{Im}\,\alpha|}\,. \tag{D.15}$$

In particular, for $\alpha \in \mathbb{R}_+$ tending to 0 one can obtain the following relation:

$$E_0(\pm z) = \sum_{n=0}^{\infty} (\pm 1)^n\, z^n = \frac{1}{1\mp z}, \qquad |z| < 1\,. \tag{D.16}$$

Because of this, for $\mathrm{Re}\alpha > 0$ the Mittag-Leffler function is an entire function. Moreover, it follows from the Cauchy inequality for the Taylor coefficients and simple properties of the Gamma-function that there exists a number $n \geq 0$ and a positive number $r(n)$ such that

$$M_{E_\alpha}(r) := \max_{|z|=r} |E_\alpha(z)| < \mathrm{e}^{r^n}\,, \forall r > r(n). \tag{D.17}$$

This means that $E_\alpha(z)$ is an entire function of finite order.

For $\alpha > 0$, by the Stirling asymptotic formula

$$\Gamma(\alpha n + 1) = \sqrt{2\pi}\,(\alpha n)^{\alpha n + \frac{1}{2}}\,\mathrm{e}^{-\alpha n}\,(1 + o(1))\;, n \to \infty\,, \tag{D.18}$$

one can see that the Mittag-Leffler function satisfies, for $\alpha > 0$, the following relations:

$$\limsup_{n\to\infty} \frac{n \ln n}{\ln \frac{1}{|c_n|}} = \lim_{n\to\infty} \frac{n \ln n}{\ln |\Gamma(\alpha n + 1)|} = \frac{1}{\alpha}\,, \tag{D.19}$$

and

$$\limsup_{n\to\infty} \left(n^{\frac{1}{\rho}} \sqrt[n]{|c_n|}\right) = \lim_{n\to\infty} \left(n^{\frac{1}{\rho}} \sqrt[n]{\frac{1}{|\Gamma(\alpha n + 1)|}}\right) = \left(\frac{\mathrm{e}}{\alpha}\right)^{\alpha}\,. \tag{D.20}$$

If $\mathrm{Re}\alpha > 0$ and $\mathrm{Im}\alpha \neq 0$, the corresponding result is valid too. Using (D.19) and (D.20) and comparing these two formulae to (D.9) and (D.10), we can say that for each α with $\mathrm{Re}\alpha > 0$ the Mittag Leffler function is an entire function of order:

$$\rho = \frac{1}{\mathrm{Re}\alpha}\,, \tag{D.21}$$

and type:

$$\sigma = 1\,. \tag{D.22}$$

In a certain sense each $E_\alpha(z)$ is the simplest entire function among those having the same order.

Bibliography

[Anderssen et al. 2004] R. S. Anderssen, S. A. Husain and R. J. Loy, The Kohlrausch function: properties and applications, *ANZIAM J.* **45** (2004), pp. C800-C816.

[Capelas et al. 2011] E. Capelas de Oliveira, F. Mainardi and J. Vaz Jr., Models based on Mittag-Leffler functions for anomalous relaxation in dielectrics, *The European Physical Journal, Special Topics* **193** (2011), pp. 161-171. Revised version in http://arxiv.org/abs/1106.1761

[Capelas et al. 2014] E. Capelas de Oliveira, F. Mainardi and J. Vaz Jr., Fractional models of anomalous relaxation based on the Kilbas and Saigo function, *Meccanica* **49** (2014), pp. 2049-2060.

[Cole et al. 1941] K. S. Cole and R. H. Cole, Dispersion and absorption in dielectrics. I. Alternating current charachteristics, *J. Chem. Phys* **9** (1941), pp. 341-351.

[Cole et al. 1942] K. S. Cole and R. H. Cole, Dispersion and absorption in dielectrics. II. Direct current charachteristics, *J. Chem. Phys* **10** (1942), pp. 98-105.

[Colombaro 2014] I. Colombaro, *Fractional Calculus and Mittag-Leffler functions*, Report for the course of Mathematical Physics, Dept. of Physics, University of Bologna, Academic year 2013/14.

[Davidson et al. 1951] D. W. Davidson and R. H. Cole, Dielectric relaxation in glycerol, propylene glycol and *n*-propanol, *J. Chem. Phys* **19** (1951), pp. 1484-1490.

[Debye 1929] P. Debye, *Polar Molecules*, Dover, Mincola, N.Y. (1929).

[Dobson et al. 1996] J. Dobson and P. Grassi, Magnetic properties of human hippocampl tissue: evaluation of artefacts and contamination sources, *Brain Res Bull* **39** (1996), pp. 255-259.

[Fröhlich 1975] H. Fröhlich, The extraordinary dielectric properties of biological materials and the action of enzymes, *Proc. Nat. Acad. Sci. USA* **72**, No. 11 (1975), pp. 4211-4215.

[Fu 2014] J. Y. Fu, On the theory of the universal dielectric relaxation, *Philosophical Magazine: Structure and Properties of Condensed Matter* **94**, No. 16 (2014).

[Gabriel 2007] C. Gabriel, Dielectric properties of biological materials, in F.S. Barnes and B. Greenebaum (Editors), *Handbook of Biological Effects of Electromagnetic Fields, 3-rd Edition. Bioengeneering and Biophysical Aspects of Electromagnetic Fields*, CRC-Taylor & Francis Group, Boca Raton, London, New York (2007), pp. 51-100.

[Gorenflo et al. 1997] R. Gorenflo and F. Mainardi, Fractional calculus: integral and differential equations of fractional order, in A. Carpinteri and F. Mainardi (Editors) *Fractals and Fractional Calculus in Continuum Mechanics*, Springer Verlag, Wien (1997), pp. 223-276.

[Gorenflo et al. 2014] R. Gorenflo, A. A. Kilbas, F. Mainardi, S. V. Rogosin, *Mittag-Leffler Functions, Related Topics and Applications*, Springer Monographs in Mathematics, Springer-Verlag, Berlin, Heidelberg (2014).

[Gripenberg et al. 1990] G. Gripenberg, S. O. Londen and O. J. Staffans, *Volterra Integral and Functional Equations*, Cambridge University Press, Cambridge (1990), pp. 143-147.

[Hanyga 2005] A. Hanyga, Physically acceptable viscoelastic models, in K. Hutter and Y. Wang (Editors), *Trends in Application of Mathematics to Mechanics*, *Ber. Math.*, Shaker Verlag GmbH, Aachen (2005), pp. 125-136.

[Hanyga et al. 2008] A. Hanyga and M. Seredyńska, On a mathematical framework for the constitutive equations of anisotropic dielectric relaxation, *J. Stat. Phys.* **131** (2008), pp. 269-303.

[Havriliak et al. 1966] S. J. Havriliak and S, Negami, A complete plane analysis of dispersion in some polymer systems, *J. Polym. Sci. Polym. Symp.* **6** (1966), pp. 99-117.

[Hilfer 2002a] R. Hilfer, Fitting the excess wing in the dielectric α-relaxation of propylene carbonate, *J. Phys.: Condens. Matter* **14** (2002), pp. 2297-2301.

[Hilfer 2002b] R. Hilfer, Analytical representations for relaxation functions of glasses, *J. Non-Cry. Sol.* **305** (2002), pp. 122-126.

[Hilfer 2002c] R. Hilfer, Experimental evidence for fractional time evolution in glass forming materials, *Phys. Rev.* **65** (2002).

[Hilfer 2002d] R. Hilfer, H-function representations for stretched exponential relaxation and non-Debye susceptibilities in glassy systems, *J. Chem. Phys.* **284** (2002), pp. 399-408.

[Hilfer 2011] R. Hilfer, Applications and impiations of fractional dynamics for dielectric relaxation, in Y. P. Kalmikov (Editor), *Recent Advances in Broadband Dielectric Spectroscopy*, Springer (2011), pp. 123-130.

[Jonscher 1983] A. K. Jonscher, *Dielectric Relaxation in Solids*, Chelsea Dielectrics Press, London (1983).

[Jurlewicz et al. 2002] A. Jurlewicz and K. Weron, Relaxation of dinamically correlated clusters, *J. Non-Cry. Sol.* **305** (2002), pp. 112-121.

[Kalmikov 2011] Y. P. Kalmikov (Editor), *Recent Advances in Broadband Dielectric Spectroscopy*, Springer (2011).

[Kalmykov et al. 2004] Y. P. Kalmykov, W. T. Coffey, D. S. F. Crothers and S. V. Titov, Microscopic models for dielectric relaxation in disordered systems, *Phys. Rev.* **70** (2004).

[Kohlrausch 1854] R. Kohlrausch, Theorie des elektrischen Rückstandes in der Leidner Flasche, *Annalen der Physik und Chemie - Poggendorff* **91** (1854), pp. 56-82, 179-213.

[Kuang et al. 1997] W. Kuang and S. O. Nelson, Low-frequency dielectric properties of biological tissues: a review with some new insights, *Transactions of the American Society of Agricultural Engineers* **41** (1997), pp. 173-184.

[Lunkenheimer et al. 2000] P. Lunkenheimer, U. Schneider, R. Brand and A. Loidl, Glassy dynamics, *Contemp. Phys.* **41** (2000), p. 15.

[Mainardi 2013] F. Mainardi, Fractional calculus and special functions, in *Lecture Notes on Mathematical Physics*, University of Bologna (2013).

[Mainardi 2014] F. Mainardi, On some properties of the Mittag-Leffler function $E_\alpha(-t^\alpha)$, completely monotone for $t > 0$ with $0 < \alpha < 1$, *Discrete and Continuous Dynamical Systems Series B* **19**, No. 7 (2014), pp. 2267-2278.

[Mainardi et al. 2014] F. Mainardi and R. Garrappa, On complete monotonicity of the Prabhakar function and non-Debye relaxation in dielectrics, *J. Comput. Phys.* **293** (2014), pp. 70-80.

[Michaelson et al. 1987] S. M. Michaelson and J. C. Lin, *Biological Effects and Health Implications of Radiofrequency Radiation*, Plenum Press, New York (1987).

[Miller et al. 2001] K. S. Miller and S. G. Samko, Completely monotonic functions, *Integr. Transf. and Spec. Funct.* **12** No. 4 (2001), pp. 389-402.

[Mittag-Leffler 1902] G. M. Mittag-Leffler, Sur l'intégrale de Laplace-Abel, *C. R. Acad. Sci. Paris*, (ser. II) **136** (1902), pp. 937-939.

[Mittag-Leffler 1903a] G. M. Mittag-Leffler, Une généralisation de l'intégrale de Laplace-Abel, *C. R. Acad. Sci. Paris*, (ser. II) **137** (1903), pp. 537-539.

[Mittag-Leffler 1903b] G. M. Mittag-Leffler, Sur la nouvelle fonction $E_\alpha(x)$, *C. R. Acad. Sci. Paris*, (ser. II) **137** (1903), pp. 554-558.

[Mittag-Leffler 1904] G. M. Mittag-Leffler, Sopra la funzione $E_\alpha(x)$, *R. Accad. Lincei, Rend.*, (ser. V) **13** (1904), pp. 3-5.

[Mittag-Leffler 1905] G. M. Mittag-Leffler, Sur la représentation analytique d'une branche uniforme d'une fonction monogene, *Acta Math.* **29** (1905), pp. 101-181.

[Nonnenmacher et al. 2000] T. F. Nonnenmacher and R. Metzler, Applications of fractional calculus techniques to problems in biophysics, in R. Hilfer (Editor) *Fractional Calculus in Physics*, World Scientific Publishing Co. Pte. Ltd., Singapore (2000).

[Novikov et al. 2005] V. V. Novikov, K. W. Wojciechowski, O. A. Komkova and T. Thiel, Anomalous relaxation in dielectrics. Equations with fractional derivatives, *Materials Science - Poland* **23**, No. 4 (2005), pp. 277-984.

[Pethig 1984] R. Pethig, Dielectric properties of biological materials: biophysical and medical applications, *Transactions on Electrical Insulation* **EI-19**, No. 5 (1984), pp. 453-474.

[Raicu 1999] V. Raicu, Dielectric dispersion of biological matter: model combining Debye-type and "universal" response, *Phys. Rev.* **60** No. 4 (1999), pp. 4677-4680.

[Schneider et al. 1999] U. Schneider, R. Brand, P. Lunkenheimer and A Loidl, Broadband dielectric spectroscopy on glass-forming propylene carbonate, *Phys. Rev.* **59** (1999), p. 6924.

[Schneider et al. 2000] U. Schneider, R. Brand, P. Lunkenheimer and A Loidl, Excess wing in the dielectric loss of glass formers: a Johari-Goldstein β-relaxation process?, *Phys. Rev. Lett.* **84** (2000), p. 5560.

[Titchmarsh 1937] E. C. Titchmarsh, *Introduction to the Theory of Fourier Integrals*, Oxford University Press, Oxford (1937).

[Williams et al. 1970] G. Williams and D. C. Watts, Non-symmetrical dielectric relaxation behavior arising from a simple empirical decay function, *Transactions of the Faraday Society* **66** (1970), pp. 80-85.

[Wikipedia HNR] Havriliak-Negami relaxation, *Wikipedia The Free Encyclopedia.*

[Wikipedia SEF] Stretched exponential function, *Wikipedia The Free Encyclopedia.*